

AD-A040 558

PRINCETON UNIV N J DEPT OF CHEMICAL ENGINEERING

F/G 7/3

THE T SUB LL RELAXATION OF POLYSTYRENE.(U)

JUN 77 J K GILLHAM, R F BOYER

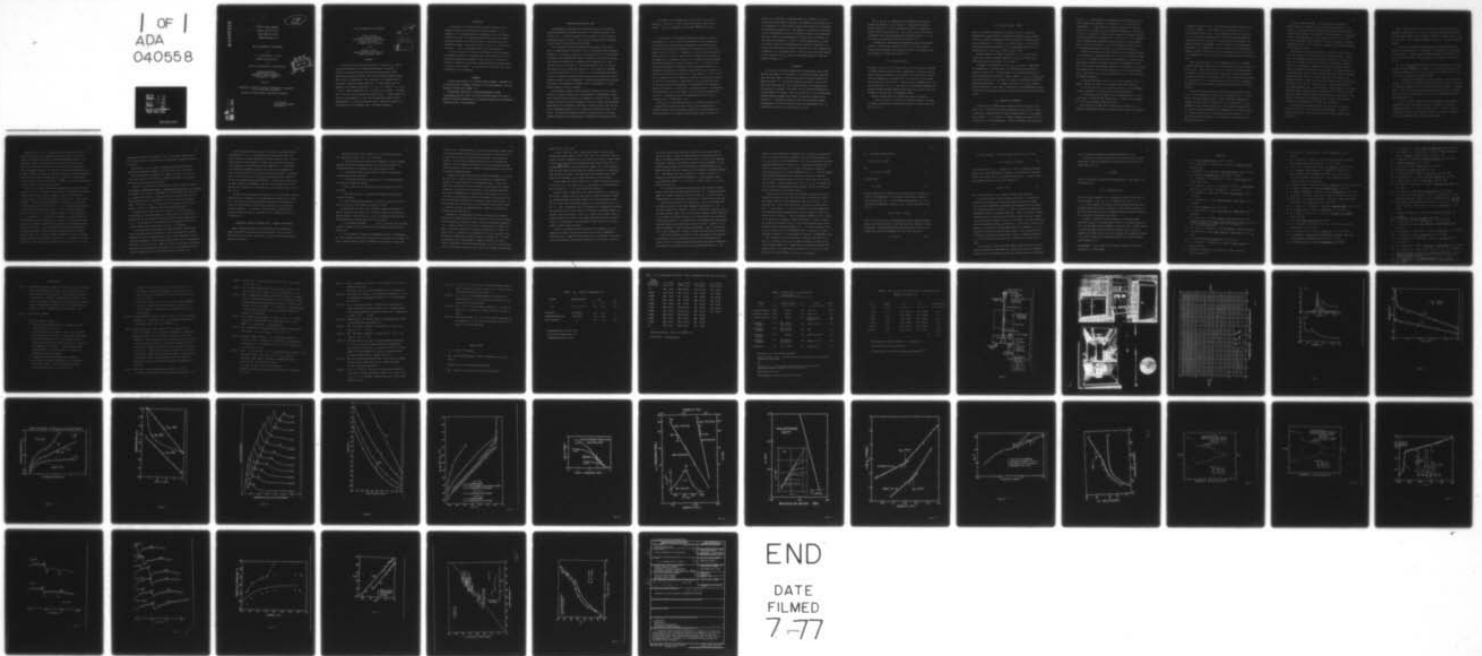
N00014-76-C-0200

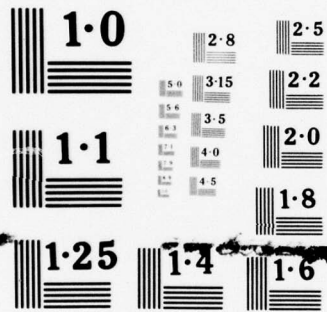
UNCLASSIFIED

TR-11

NL

1 OF 1  
ADA  
040558





NATIONAL BUREAU OF STANDARDS  
MICROCOPY RESOLUTION TEST CHART

AD A 040558

1473

12

OFFICE OF NAVAL RESEARCH

Contract N0014-76-C-0200

Task Number NR 356-504

TECHNICAL REPORT NO. 11

THE  $T_{\alpha\alpha}$  RELAXATION OF POLYSTYRENE

by

J. K. Gillham and R. F. Boyer

Accepted for Publication

in

Journal of Macromolecular Science-Physics

Princeton University  
Polymer Materials Program  
Department of Chemical Engineering  
Princeton, N. J. 08540

June 1977

Reproduction in whole or in part is permitted for any purpose  
of the United States Government

Approved for Public Release; Distribution Unlimited.

DDC  
JUN 15 1977  
C

AD No. \_\_\_\_\_  
DDC FILE COPY.

J. K. Gillham  
Principal Investigator  
609/452-4694



## INTRODUCTION

The existence of a relaxation above the glass transition ( $T_g$ ) in amorphous polymers has been reported by numerous authors (e.g. 1-5). Agreement on its interpretation has not developed; in fact its existence has been questioned. The evidence has been elusive since some investigators have observed it and others have not -- even when using similar experimental methods. Boyer has referred to it as the  $T_{ll}$  liquid-liquid transition since the phenomenon occurs in the liquid phase (1).

A review of recent work (5-13) by the authors and their colleagues on amorphous polystyrene is presented from a chronological point of view. The approach emphasizes development of their own work, the question of whether the relaxation is molecularly and/or macroscopically based and how it relates to the literature. In particular, it sets the stage for further investigation of the controversy.

## MATERIALS

"Anionic" polystyrenes [(5), Pressure Chemical Company, Pittsburgh, Pa.] and fractions from a "thermal" polystyrene (5) have been examined. All were designated "monodisperse" ( $\bar{M}_w/\bar{M}_n \approx 1.1$ ).

The particular plasticizer, m-bis(m-phenoxyphenoxy) benzene,  $[(C_6H_5OC_6H_4O)_2C_6H_4]$ ; MW = 446.5, BP 273-276°C/1 mm Hg pressure] was used (7) because of the known compatibility of a polymeric analogue, poly(2,5-dimethyl-1,4-phenylene oxide), with polystyrene.

## TORSIONAL BRAID ANALYSIS (TBA)

Thermomechanical experiments were performed using a fully automated torsional pendulum which operates at about 1 Hz throughout the range -190° to 400°C (14). A schematic diagram of the instrument is shown in Figure 1; photographs appear in Figure 2. This torsional pendulum has been developed under the name "torsional braid analysis" (TBA).

The instrument intermittently generates freely damped waves each of which is characterized by the period ( $P$ , sec.) of oscillation and logarithmic decrement [ $\Delta = \ln(A_i/A_{i+1})$ , where  $A_i$  is the amplitude of the  $i$ th oscillation]. A computer plots thermomechanical spectra consisting of the Relative Rigidity and Logarithmic Decrement of the specimen versus temperature (or time) in immediate time on an XY plotter: the Relative Rigidity ( $1/P^2$ ) is directly proportional to the in-phase shear modulus ( $G'$ ); the Logarithmic Decrement is directly proportional to  $G''/G'$ , where  $G''$  is the out-of-phase shear modulus.  $G'$  and  $G''$  are material parameters which characterize the storage and loss of mechanical energy on cyclic deformation. Transition temperatures are assigned from peaks in the logarithmic decrement (which are accompanied by corresponding changes in relative rigidity).

Each composite specimen of TBA was prepared generally from a 10 percent solution (g. weight polystyrene/ml. volume benzene) by impregnating a glass braid, mounting and then heating in the apparatus in helium to 200°C. Thermomechanical spectra were usually obtained in helium on cooling from the maximum temperature used in preparing the specimen to below the glass transition and then on subsequent heating to 200°C. Heating and cooling rates were 1.5°C/minute. The absence of hysteresis effects on repeated runs with the same specimen suggests that residual solvent is negligible after heating to 200°C.

As an example of the thermomechanical spectra which were used to measure  $T_g$ ,  $T_{\min}$  and  $T_{\ell\ell}$ , Figure 3 shows TBA data for a sample of polystyrene.  $T_{\min}$  is the temperature of minimum loss<sup>( $\Delta$ )</sup> between  $T_g$  and  $T_{\ell\ell}$ .

$G''$  rather than  $\Delta$  is the preferred function for assigning values of transitions [ $G'' \approx G'(\Delta/\pi)$ ], since energy losses due to the relaxations of the transitions in dynamic mechanical experiments are characterized explicitly by  $G''$  and since the temperature of the maximum in loss for  $G''$  is equal to that of  $dG'/dT$  (15). A comparison of various modes for presenting mechanical loss [ $\Delta$ ,  $G''$  and  $\alpha$ , where  $\alpha$  is the exponential decay constant of the damped wave] is presented in Figure 4 for a composite polystyrene/glass braid specimen through the  $T_g$  and  $T_{\ell\ell}$  regions (16). It is noted in this case that representation of mechanical loss by logarithmic decrement, as automatically plotted by the instrument, exaggerates the  $T_{\ell\ell}$  loss peak, for example, by decreasing the intensity of  $\Delta$  at  $T_{\min}$  because  $\Delta \approx \pi G''/G' \sim \pi G''/P^2$  and  $P$  increases with rise in temperature (particularly through the  $T_g$  region).  $T_{\ell\ell}$  by the  $G''$  representation is weak compared with  $T_g$  and might be missed in some types of physical measurements. The temperature of the maximum in mechanical loss for  $T_{\ell\ell}$  is higher for  $\Delta$  in comparison with  $G''$ . The magnitude of the effect for  $T_{\ell\ell}$  is seen in Table 1 for three different polymer fractions (16). The numerical value of the temperature for  $T_g$  is also increased by use of  $\Delta$  rather than  $G''$  (15).

Above  $T_{\min}$  (17) for unfilled polymers it is generally considered that  $G'$  decreases at a greater rate than  $G''$  with increasing temperature at constant frequency (or with decreasing frequency at constant temperature), and therefore that  $G''/G'$  increases without passing through a maximum. In

contrast  $T_{\ell\ell}$  is assigned in a TBA experiment from a *maximum* in  $\Delta$  of the polymer/glass fiber composite specimen. This maximum could be argued to be the consequence of  $G'$  not decreasing significantly because of the elasticity of the supporting substrate (8). The maximum in  $\Delta$  would then be considered to arise from macroscopic flow of the polymeric material, which would probably occur relative to the substrate at a certain level of viscosity. On this basis of the maximum in  $\Delta$  (and  $G''$ ) in the TBA experiments,  $T_{\ell\ell}$  would not therefore represent the manifestation of a molecular transition.  $T_{\ell\ell}$  would be certified as being a molecular transition if it were accompanied by a maximum in  $G''$  in the polymer itself. It will be shown later that analysis of the literature in the  $T_{\ell\ell}$  region of polystyrene appears to reveal the presence of maxima in  $G''$ .

#### TBA RESULTS

The  $T_g$  and  $T_{\ell\ell}$  transition temperatures for monodisperse anionic polystyrenes are plotted vs.  $1/M$  (Figure 5). The curves were drawn using TBA data; DTA ("DSC" DuPont) results obtained using particulate samples were added (see later) (5). The  $T_g$  plot indicates two regions, each of which follows the relationship  $T_g = T_g^\infty - K_g M^{-1}$  where  $T_g^\infty$  is the maximum value of  $T_g$  and  $K_g$  is a constant. The plot of the  $T_{\ell\ell}$  transition temperature vs.  $1/M$  also displays two regions. Plots of  $T_{\ell\ell}$  and  $T_g$  vs.  $1/M$  for fractionated thermal polystyrene samples were similar to those for the anionic polystyrenes (5). The molecular weight at which the relationships changed corresponded to the critical molecular weight for entanglements ( $M_c$ ). It was noted that  $M_c$  for  $T_{\ell\ell}$  is less than  $M_c$  for  $T_g$  (5).

The  $T_g$ ,  $T_{\min}$  and  $T_{\ell\ell}$  temperatures for monodisperse anionic polystyrenes are plotted vs.  $\log M$  (Figure 6). Throughout the range of molecular weights ( $M \geq M_c$ ) the corresponding results for thermal polystyrene fractions were similar (5). The  $T_g$  and  $T_{\ell\ell}$  plots are similar to isoviscosity plots relating temperature to molecular weight (5). It is seen that  $T_{\min}$  varies linearly with  $\log M$  above  $M \approx 10^4$ .

Investigation of binary blends of monodisperse anionic polystyrenes showed (6) that when both components have  $M < M_c$ , both the  $T_g$  and  $T_{\ell\ell}$  transitions were averaged, and an equation similar to that commonly used for averaging  $T_g$  (18) was also obeyed for  $T_{\ell\ell}$ :

$$1/T_{\ell\ell} \approx W_A/A T_{\ell\ell} + W_B/B T_{\ell\ell}$$

where  $A T_{\ell\ell}$ ,  $B T_{\ell\ell}$  and  $T_{\ell\ell}$  are values of the  $T_{\ell\ell}$  ( $^{\circ}\text{K}$ ) transition for polymer A, polymer B and the blend of A and B, respectively, and  $W_A$  and  $W_B$  are the weight fractions of polymers A and B, respectively, in the blend. Further, when both components of the blends have  $M < M_c$ ,  $T_g$  and  $T_{\ell\ell}$  of the blends vary linearly with  $1/\bar{M}_n$  (Figure 7). However, when one component has  $M < M_c$  and the other has  $M > M_c$ ,  $T_{\ell\ell}$  transitions of the individual components are observed although the glass transition has single values which result from averaging in the usual way for homogeneous blends.

Results (Figures 8 and 9) on plasticized anionic polystyrene

show (7) that the  $T_{\ell\ell}$  transition is observed throughout the range of composition and follows an equation which again is similar to that used for  $T_g$  (18), i.e.

$$T_{\ell\ell} = A^{T_{\ell\ell}} W_A + B^{T_{\ell\ell}} W_B + K W_A W_B$$

where  $K$  is an empirical constant,  $A^{T_{\ell\ell}}$  and  $W_A$  are the  $T_{\ell\ell}$  transition temperature and weight fraction of the pure polystyrene, and  $B^{T_{\ell\ell}}$  and  $W_B$  are the  $T_{\ell\ell}$  transition temperature and weight fraction of the pure plasticizer, respectively.  $K = -59.6^\circ\text{K}$ ,  $A^{T_{\ell\ell}} = 424^\circ\text{K}$  and  $B^{T_{\ell\ell}} = 274^\circ\text{K}$  for the particular plasticizer/polystyrene. The corresponding values for the  $T_g$  transition are  $K = -111^\circ\text{K}$ ,  $A^{T_g} = 380^\circ\text{K}$  and  $B^{T_g} = 255^\circ\text{K}$ .

Another relaxation is observed (Figure 8,  $T_{\ell\ell}' > T_{\ell\ell}$ ) which varies linearly with weight percentage composition, with  $A^{T_{\ell\ell}'} = 484^\circ\text{K}$ ,  $B^{T_{\ell\ell}'} = 289^\circ\text{K}$  and the empirical constant  $K = 0$  (Figure 9).

A summary of the TBA data on the  $T_g$ ,  $T_{\min}$ ,  $T_{\ell\ell}$  and  $T_{\ell\ell}'$  temperatures for homopolymers (5), polymer blends (6) and plasticized polystyrene (7) appears in Figure 10 (8). Numerical data for the plasticized polystyrene which were omitted from reference 7 appear in Table 2.  $T_{\ell\ell}$ ,  $T_{\ell\ell}'$  and  $T_{\min}$  ( $^\circ\text{K}$ ) are plotted versus  $T_g$  ( $^\circ\text{K}$ ) in Figure 10 to explore relationships between the relaxation temperatures. It is apparent that the ratio  $T_{\ell\ell}/T_g$  is approximately constant over a wide range of temperature for the homopolymers, binary blends and the plasticized polystyrene, except above  $M_c$  and at high plasticizer content.

#### $T_{\ell\ell}$ : RHEOLOGICAL LITERATURE

Consider first the dynamic melt viscosity data of Cox, Nielsen, and Keeney (19) on a polystyrene fraction of molecular weight 240,000. Figure 2 of reference 19 combines both the in-phase dynamic modulus,  $G'$ , and dynamic melt viscosity,  $\eta'$  ( $= G''/\omega$  where  $\omega$  is angular frequency in radians  $\text{sec}^{-1}$ ), as a function of  $\omega$  at four temperatures. Figure 11 reproduces only the shapes

of the  $\eta' - \omega$  log-log plots at four temperatures and extends them at the high frequency end according to the dashed lines. It is seen that the extrapolated  $\eta' - \omega$  plots intersect, giving the impression of identical values of  $\eta'$  at the same  $\omega$  but at two different temperatures. This can be true only if a crossplot at fixed  $\omega$  shows a plateau or a maximum. The inset to Figure 12 shows such a cross-plot at  $\omega = 5 \text{ rad. sec.}^{-1}$ . It is suggested that the maximum shown (admittedly based on a paucity of points) corresponds to  $T_{\ell\ell}$  at that frequency.  $T_g$  at this frequency lies well below the four temperatures employed, and hence, this loss peak lies above  $T_g$ .

Maxima can be estimated in similar fashion at other frequencies permitting construction of a relaxation map,  $\log f - 1/T$  ( $^{\circ}\text{K}$ ), as shown in Figure 12 ( $f = \text{Hz}$ ). Although only 3 points can be estimated with confidence, the data suggest an apparent enthalpy of activation of approximately 30 Kcal mole $^{-1}$  which agrees with measurements made for us by Burmester (20) on anionic polystyrene with  $\bar{M}_n = 37,000$  using a Rheovibron. The latter data suggest  $\Delta H_a \approx 33 \text{ Kcal mole}^{-1}$  for  $T_{\ell\ell}$  and 130 Kcal mole $^{-1}$  for  $T_g$ . Three conclusions are immediately apparent.

a) The data obtained by Cox et al. (19), when considered in the  $\eta' - T$  domain, indicate the presence of a relaxation process lying above  $T_g$ .

b) The  $\Delta H_a$  value for  $T_{\ell\ell}$  is lower than  $\Delta H_a$  for  $T_g$ . This is probably a direct consequence of the larger free volume present above  $T_g$ .

c) The straight line of Figure 12 can be extrapolated to  $f = 0.3 \text{ Hz} = 1.88 \text{ rad/sec}$ , the effective TBA frequency at  $T_{\ell\ell}$ . From this one estimates  $T_{\ell\ell} = 167^{\circ}\text{C}$  for a molecular weight of 240,000.

Next consider the dynamic melt viscosity data of Onogi et al. (21) obtained on polystyrene fractions of various molecular weights as a function

of angular frequency at 200°C. Their data are reproduced schematically in the inset to Figure 13. The straight line for zero shear rate,  $\omega = 0$ , has the expected slope of 3.4. Other frequencies tend to show a maximum in  $\eta'$  as a function of molecular weight. Although the maxima cannot be located with precision, Figure 13 is a log-log correlation between  $\omega$  and molecular weight at the maximum. One can then make the relatively short extrapolation to a frequency of 0.3 Hz = 1.88 rad sec<sup>-1</sup> and estimate the maximum in dynamic viscosity to occur at a molecular weight of ca. 560,000. It is suggested that the  $T_{\ell\ell}$  of PS for this molecular weight and frequency is 200°C.

Other results by Onogi et al. which appear to bear on  $T_{\ell\ell}$  phenomena have been published elsewhere (22, 23) and reproduced in part in Figure 13.13 by Ferry (24). These latter results (22, 23) are on anionic polystyrenes in contrast to the earlier (21) data on fractions of thermal polystyrenes. Using the anionic data, all reduced to 160°C, and the above procedure results in a log-log plot of  $\omega$  vs. molecular weight which also gives a reasonably straight line. One can estimate a molecular weight of 68,000 as giving  $T_{\ell\ell}$  at 160°C.

The capillary zero shear melt viscosity data on polystyrene by West et al. (25) is represented in Figure 14 as a conventional  $\log \eta - 1/T$  plot. There is an abrupt change in slope at 168°C, below which temperature we estimate  $\Delta H_a = 58$  Kcal mole<sup>-1</sup>, above which  $\Delta H_a = 30$  Kcal mole<sup>-1</sup>, in good agreement with  $\Delta H_a$  values from Figure 12. It is therefore suggested that  $T_{\ell\ell}$  for this polymer corresponds to the temperature of the break in Figure 14. Similar conclusions can be drawn from the data of Karam et al. (26) which are also shown in Figure 14. Not plotted are similar data from Spencer and Dillon (27).

Figure 14 raises two issues. The first concerns what effective dynamic frequency to associate with the steady shear parameter,  $\eta_0$ . Obviously  $\eta_0$  is a derived quantity obtained by extrapolating viscosity data at finite rates of shear. Data supplied by the authors show  $\eta$  is relatively constant and assumed equal to  $\eta_0$  up to shear rates of  $10^{-2}$  to  $10^{-3} \text{ sec}^{-1}$ . If we take this range to be equivalent to the lowest frequency in a dynamic experiment at which  $\eta$  is not a function of frequency, the effective frequency is well below that of TBA.

Discussion of the second issue follows. Convention informs us that a plot such as that in Figure 14 must curve monotonically upward. However, there is no ambiguity about the two straight line sections in Figure 14, a fact which the reader may verify by plotting the original data. Moreover, Utracki (4) has conducted a computer fit of real melt viscosity data on a variety of systems to various continuous functions. He invariably found one or two temperature regions in which systematic deviations from the continuous function are found. One can, of course, draw some kind of smooth curve through the points in Figure 14, but the best overall fit will show systematic deviations of the same sign in the  $T_{\ell\ell}$  regions. Some analogy may be made with thermal expansion data. The coefficient of cubical expansion  $\alpha(\text{cc/cc/deg})$  tends to increase over broad ranges of temperature as  $T^{1/2}$  and yet on either side of  $T_g$  there is a short linear range connected by a curved section. This behavior is considered to be normal at  $T_g$  and, in fact, at some secondary relaxations in the glassy state [see Ref. (28) for details].

Hyun (29) has investigated capillary flow on an atactic polystyrene of  $\bar{M}_w = 250,000$ ,  $\bar{M}_n = 107,000$  using an Instron Rheometer. A change in character of the flow at  $180^\circ\text{C}$  was noted which the author suggested might relate to  $T_{\ell\ell}$ .

Table 3 collects values of  $T_{\ell\ell}$  as a function of the molecular weight of monomodal distributions at  $f \approx 0.3$  Hz for a series of polystyrenes measured by conventional methods of melt rheology. Values of  $T_{\ell\ell}$  from  $\eta_0$  and at 3.5 Hz are also given. These results are plotted in Figure 15. Several conclusions emerge.

a) The overall agreement between conventional rheological data and TBA data is quite good for  $M > M_c$  especially in consideration of the diverse sources of data. It appears that polydisperse samples give a better fit if  $\bar{M}_w$  is used rather than  $\bar{M}_n$ . The  $\bar{M}_n$  correlation of reference 6 held only for  $M < M_c$ .

b) The capillary rheometer values of  $T_{\ell\ell}$  are consistently low as might be expected for their<sup>low</sup> effective frequency. It has been noted that use of the logarithmic decrement function for the assignment of numerical values to  $T_{\ell\ell}$  also shifts it to higher temperatures by TBA.

c) Conventional melt rheometry, like TBA, detects  $T_{\ell\ell}$  at high molecular weights ( $> M_c$ ) (TBA has given weak loss peaks above  $MW = 100,000$ ). Onogi and his coworkers suggested that their loss peaks arise from slippage of entanglements. Unlike the results of TBA there does not appear to be a  $T_{\ell\ell}$  dynamic melt viscosity peak in references 21, 22 and 23 for polystyrene with low molecular weight ( $< M_c$ ).

d) There is still a question as to why some types of melt viscosity measurements give no indication of  $T_{\ell\ell}$  as, for example, in the data of Plazek and O'Rourke (31). The low intensity of  $T_{\ell\ell}$  as seen in  $G''$  versus frequency plots (e.g. Figure 4) may be a factor.  $T_{\ell\ell}$  might be considered as a minor perturbation on a strong melt flow process.

Ueberreiter et al. (3, 32, 33) obtained a plot similar to that of  $T_{\ell\ell}$  versus  $\log M$  of Figure 11 by measuring a flow transition, " $T_F$ ", of polystyrene in particulate form using a fixed-load penetrometer method. [The terminology, "glass", "fixed fluid" and "true liquid" which is used in Figure 6 was introduced by Ueberreiter for designating the main physical states of amorphous polymers.] The  $T_F$  plot for fractionated polystyrene (33) is shown in Figure 16 together with TBA data points for  $T_{\ell\ell}$  taken from Figure 6. Ueberreiter and Orthmann concluded that the  $T_F - \log M$  plot represented an isoviscous state, just as has been shown (5) for <sup>the</sup>  $T_{\ell\ell} - \log M$  plot (see also the later discussion in connection with Figure 25).

There is a new genre of visco-elastic phenomena having to do with block copolymers (34, 35). For example, Chung and Gale (34) investigated a styrene-butadiene-styrene (SBS) triblock copolymer for which the S blocks had a molecular weight of 7000, and the B blocks a value of 43,000 using a rheogoniometer. Marked non-Newtonian behavior was observed at 125, 140, and 150°C but Newtonian flow occurred at 175°C.  $T_{\ell\ell}$  for homopolymer polystyrene of this molecular weight is about 147°C at 0.3 Hz. One notes from their Figure 2 (34) that the 175°C line crosses the plots for lower temperatures at  $\omega \approx 10^2$  rad/sec or  $f \approx 16$  Hz for which frequency  $T_{\ell\ell}$  would be above 147°C. The explanation given by the authors for the change in viscoelastic behavior was that the two-phase system below 150°C becomes a single homogeneous phase between 150 and 175°C.  $T_g$  of the low molecular weight polystyrene phase in an SBS block copolymer is lower than that of homopolystyrene of the same molecular weight (36). An earlier dynamic mechanical loss study on styrene-ethylene oxide diblock copolymers by Erhardt et al. (35) showed a loss ( $\tan\delta$ ) peak at about 100°C ( $T_g$ ) and one at about 160°C (both at 3.5 Hz) for a block

copolymer whose styrene block had  $\bar{M}_n = 47,000$ . The authors suggested that the loss peak at  $160^\circ\text{C}$  is associated with establishment of phase equilibrium in the melt.

These results (34, 35) cannot be compared directly with TBA data at similar molecular weights because of the single free end of the S block.

DSC on an SBS triblock copolymer (13) appears to reveal a  $T_{\ell\ell}$  for the S block ( $\bar{M}_n = 14,000$ ) at  $152^\circ\text{C}$  which is somewhat higher than  $T_{\ell\ell}$  for anionic polystyrene of the same molecular weight.

TBA data for two SBS triblock copolymers are shown in Figures 17 and 18 (Gillham-Boyer, unpublished results). (Experimental details and a list of transitions appear on the figures). Assignments of the glass transition ( $T_g$ ) and  $T_{\ell\ell}$  relaxation attributed to the polystyrene blocks are both lower for the block copolymers than for homopolymers of the same polystyrene molecular weight. The ratio  $T_{\ell\ell}/T_g = 1.1$  for these block copolymers and for homopolymers of styrene of comparable polystyrene molecular weight (5).

We propose herein that if there is structure in the fluid of polystyrene above  $T_g$ , then establishment of a single phase in a styrene block copolymer may not be achieved until the polystyrene structure breaks up at  $T > T_{\ell\ell}$ . Investigations of the morphology versus temperature should distinguish between the two propositions for the  $T > T_g$  relaxation.

It was noted above that although high molecular weight narrow distribution polystyrene shows a maximum in  $G''$  versus log frequency at constant temperature at lower frequencies than for  $T_g$  ( $\equiv$  higher temperatures than  $T_g$  at constant frequency), lower molecular weight polymers show no corresponding maximum in  $G''$  (21, 22, 23, 24). However, blends of low molecular weight/high molecular weight polymer display shoulders in  $G''$  versus frequency which are directly attributable to the low molecular weight constituent (24).

Analogous dynamic mechanical spectra of blends of low molecular weight polybutadiene ( $\bar{M} > M_c$ ) in high molecular weight polybutadiene ( $\bar{M} \gg M_c$ ) versus frequency at constant temperatures displayed maxima in  $\tan\delta$  ( $= E''/E'$ , where E refers to tensile moduli) at longer time scales than for  $T_g$  which were attributed to the low molecular weight component (2). The locations of the maxima were dependent on molecular weight but were independent of amount; the intensities of the loss peaks increased with amount. It was also shown (2) that the value of  $\tan\delta$  at  $T_{\min}$  was determined by  $\bar{M}_n = 1440/\tan^2\delta$  for both the unmixed and mixed polybutadienes. This provides evidence that the mixed systems were homogeneous. The energy of activation for the loss maximum was 11 Kcal/mole (2); we estimate for cis polybutadiene  $\Delta H_a \approx 20$  Kcal/mole for  $T_g$ .

This mixing without averaging of frequency ( $\equiv T$ ) for polystyrene and polybutadiene blends is analogous to the homopolymer/glass blend results of TBA, and to the high molecular weight polymer/low molecular weight polymer TBA results for blends where the low molecular weight species "show through" without averaging (6). In contrast, when both polymer constituents have molecular weights less than  $M_c$ , averaging of the  $T_{\ell\ell}$  temperatures occurs in the TBA data (6).

#### DIFFERENTIAL SCANNING CALORIMETRY (DSC): RESULTS AND DISCUSSION

Results obtained using DTA and DSC techniques can be interpreted to support and extend the conclusions obtained using TBA. Just as for TBA, a problem exists as to whether the data for  $T_{\ell\ell}$  arise from a molecular and/or a macroscopic relaxation.

Observations by DTA ("DSC", DuPont) on  $T_{\ell\ell}$  of anionic polystyrenes were reported by Stadnicki et al. (5) as follows:

1. Initial heating runs on particulate (powdered or fibrous) polymer samples revealed two endothermic peaks, one at  $T_g$  and the other at  $T_{\ell\ell}$ , both agreeing within a few degrees with values obtained by TBA.

2. On reheating (after cooling from 200°C to RT), a single event corresponding to  $T_g$  was observed.

3. If the resulting film was powdered at RT, two endothermic peaks would again be observed on heating.

4. The  $T_{\ell\ell}$  event was not observed for molecular weights of 110,000 and higher.

5. The intensity of the  $T_{\ell\ell}$  endotherm was maximum at heating rates of about 40°C/minute.

6. After heating powdered polymer to just above  $T_g$  and cooling to RT, both the  $T_g$  and  $T_{\ell\ell}$  events showed on reheating to 200°C.

It was evident that the  $T_{\ell\ell}$  thus observed on powder resulted from a type of "melting" of the atactic PS, with sudden wetting of the pan and an apparent change in specific heat,  $C_p$ . This  $T_{\ell\ell}$  endothermic peak might have been dismissed as an artifact were it not for two facts:

1.  $T_{\ell\ell}$ -log MW by DTA agreed with  $T_{\ell\ell}$ -log MW by TBA, including a change in slope at  $M_c$ , the critical molecular weight for chain entanglement (Fig. 6).

2. It also agreed in character and temperature with  $T_F$ , the temperature of fusion, reported on particulate polystyrenes by Ueberreiter and Orthmann (33), using a totally different type of instrument in which fusion occurred under

load (Fig. 16). Visual observation on particulate polystyrene samples using a hot stage microscope showed that fusion occurred over a range of 5-10°C in the vicinity of the  $T_{\ell\ell}$  transition, being sharper at lower molecular weights. Since this was a no-load (save gravity) test, as was DTA, the sharpness of fusion suggested the existence of a basic molecular mechanism which was obscured in DTA by the artifact of improved wetting of the pan and the resulting endothermic peak.

A sharp step or peak in DTA and DSC is often a consequence of a  $\Delta C_p$  such as occurs at  $T_g$ . Here  $\Delta C_p$  arises from hole formation, as elaborated by Kauzmann (37), Hirai and Eyring (38) and Wunderlich (39). O'Reilly and Karasz (40) noted that there was no observed  $\Delta C_p$  associated with secondary relaxations in the glassy state of polymers. These secondary relaxations were usually accompanied by a relatively small discontinuity,  $\Delta\alpha$ , in coefficient of cubical expansion, reported by Heydemann and Guicking (41) for PVC and PMMA and by Simha and his colleagues for many polymers (42-44). It seems possible that the change in  $C_p$  to be expected with such small changes in  $\alpha$  might be too weak to be observed by DSC. However, an alternate explanation has been proposed (45).

Examination of the published literature on observations of secondary transitions by thermal means led to the conclusion that  $C_p$ -T plots exhibited not a discontinuity in  $C_p$  but a change in slope at the secondary relaxations (45). A change in slope of a  $C_p$ -T curve is a discontinuity in  $d^2H/dT^2$ , and hence a third order transition in the sense of Ehrenfest (46). Figure 19 shows a plot of  $C_p$  against T for a butadiene-22.6% styrene copolymer, using the precision thermal data of Rnads, Fergusson, and Prather (47). Although the data above  $T_g$  were represented by a quadratic equation, two linear regions intersecting at 269°K have been considered (45) to be a more realistic fit of the actual data, especially since other similar examples were available

(Tables 1 and 2 of Ref. 45).

In view of this, DSC ("DSC", Perkin Elmer) traces of anionic polystyrenes after being heated to 200°C, held at 200°C for 15 minutes, and then cooled to RT were re-examined with the finding that a change in slope occurred in every case on fused films at temperatures which agreed closely with  $T_{\ell\ell}$  assignments made by TBA and from DSC data on powders (12). These changes in slope had been ignored as being base-line changes, especially as endothermic peaks had been anticipated. New experiments were performed using a Perkin Elmer DSC 1B instrument at 40°C/minute, discussion of which follows.

The DSC results are shown in Table 4(12). Repeat runs show more scatter in  $T_{\ell\ell}$  than in  $T_g$ . The ratios of  $T_{\ell\ell}$  to  $T_g$  are equal to 1.16 which extends earlier results (2, 6, 7) in that the ratio holds above  $M_c$ .

Figure 20 shows a comparison of DSC traces on powder and on fused film, and Figure 21 compares traces on fused films at different molecular weights.  $T_{\ell\ell}$  on powder becomes increasingly weaker with increasing molecular weight, and is no longer seen at molecular weights of 110,000 and higher (Fig. 5 of Ref. 5). This is undoubtedly a direct consequence of increased melt viscosity which decreases the flow and results in non-wetting of the sample holder. In contrast, one notes from Fig. 21 that  $T_{\ell\ell}$  is clearly seen on fused film at a molecular weight of 2,000,000. The slightly diminished intensity is mainly a result of less material in the pan because of poor packing of the fluffy powder at higher molecular weights.

Thus it is concluded that the intensity of the relaxation of  $T_{\ell\ell}$ , as judged by the change in slope of the DSC trace, is almost independent of molecular weight. Indeed, one might expect this if a molecular level process such as the breaking of weak secondary bonds at  $T_{\ell\ell}$  is involved. Figure 22

is a plot of DSC values on fused films with DTA values on powder and TBA results from Ref. 5. There are small differences in molecular weight for some of the samples between the two sets of data. One sees a very important distinction: above  $M_c$ , the molecular weight for chain entanglement,  $T_{\ell\ell}$  for powder increases rapidly since a flow process is involved whereas  $T_{\ell\ell}$  on fused films levels off just as does  $T_g$  as the influence of end groups diminish (12). The limiting value of  $T_{\ell\ell}$  from Fig. 22 is seen to be 435°K. In analogy with the glass transition temperature, a single equation relates  $T_{\ell\ell}$  to molecular weight, i.e.,  $T_{\ell\ell} = T_{\ell\ell}(\infty) - K_{\ell\ell} \bar{M}_n^{-1}$ , where  $T_{\ell\ell}(\infty)$  is the limiting value of  $T_{\ell\ell}$ .

It is therefore concluded on general grounds, and confirmed by experimental results, that the liquid-liquid transition,  $T_{\ell\ell}$ , in polystyrene should appear as a change in slope on the DSC trace above  $T_g$ . It has the general characteristics of a third order transition and is therefore relatively weak.

Concern that TBA values of  $T_{\ell\ell}$  might arise in part as an artifact from the composite nature of the polymer impregnated glass braid (6, 7) was initially enhanced by an inability to obtain an endothermic response by DTA once the powder had been fused. This concern has been lessened by cross-comparison of  $T_{\ell\ell}$  results with rheological data of the literature and by the conclusions of the present section. In a broader sense, the endothermic DTA peak observed with particulate anionic polystyrenes is not an artifact. Instead, it is a specific response to a specific molecular mechanism. Since it involves melt flow, it must change at  $M_c$ . Below  $M_c$  it agrees with DSC data on fused films.

These results obtained using DSC on fused films parallel those obtained by Ueberreiter and his collaborators who found that thermal diffusivity (units of  $\text{cm}^2 \text{sec}^{-1}$ ) showed two abrupt drops when plotted against temperature for fractions of polystyrene (48) and of polymethylmethacrylate (3). The

decrease at lower temperature corresponds with  $T_g$  obtained by conventional means; the decrease at higher temperature seems to be a manifestation of  $T_{\ell\ell}$ . The ratio of the two temperatures (in °K) was constant above and below  $M_c$  (polymethylmethacrylate fractions, 3). The authors showed that the decreases in thermal diffusivity is a result of decreases in modulus of elasticity at  $T_g$  and at the higher temperature (our  $T_{\ell\ell}$ ). This also suggests a basic molecular mechanism since no macroscopic motion or "melting" is involved in the thermal diffusivity tests which were carried out on fused rods of polymer. Figure 23 shows plots of  $T_{\ell\ell}$  vs.  $T_g$  (°K) for thermal diffusivity data on polymethylmethacrylate fractions (3) and for TBA data on anionic polystyrenes (5) and their blends (6).

Duda and Vrentas (49) measured the diffusion of n-pentane in atactic commercial polystyrene of  $\bar{M}_w = 412,000$  ( $\bar{M}_n$  was not reported but would be approximately 200,000) in the temperature range of 140 to 170°C. A log diffusion rate - 1/T plot has two straight line portions intersecting at 150°C. A log solubility - 1/T plot also changes at the same temperature. This temperature agrees reasonably well with the asymptotic value of  $T_{\ell\ell}$  by DSC as seen in Figure 22. Chain entanglements apparently have no effect on the diffusion of n-pentane. Additional examples of a similar change in the character of diffusion near  $T_{\ell\ell}$  in three other polymers and six other penetrants will be discussed elsewhere (50). It has been argued (51) that  $T_{\ell\ell}$  has a kinetic but not a thermodynamic basis. Diffusion is a kinetic phenomenon, solubility is an equilibrium one and hence a thermodynamic event.

The generality of the  $T_{\ell\ell}$  transition is apparent from Figure 24 in which  $T_{\ell\ell}$  is plotted versus  $T_g$  for a number of atactic and quenched semi-crystallizable polymers (13). These results were obtained using DSC techniques as above. It follows from the constant ratio,  $T_{\ell\ell}/T_g = 1.2$ , that molecular architecture affects  $T_{\ell\ell}$  and  $T_g$  in the same way.

$T_{\ell\ell}$ : An Iso-Free Volume State (11)

$$\text{If } T_g = T_g(\infty) - K_g \bar{M}_n^{-1} \quad (1)$$

and

$$T_{\ell\ell} = T_{\ell\ell}(\infty) - K_{\ell\ell} \bar{M}_n^{-1} \quad (2)$$

it follows that

$$T_{\ell\ell} = K_4 T_g \quad (3)$$

where the subscript 4 is employed to avoid confusion with constants  $K_1$  to  $K_3$  used in the Simha-Boyer (52) discussion of free volume. Equation 3 holds for polystyrene ( $K_4 \approx 1.2$ ) and polymethylmethacrylate ( $K_4 \approx 1.24$ ). Free volume at temperature  $T$  above  $T_g$ ,  $V_f(T)$ , increases according to WLF (53) as:

$$V_f(T) = V_f(T_g) + \Delta\alpha(T - T_g) \quad (4)$$

where  $\Delta\alpha$  is the difference in coefficients of cubical expansion above and below  $T_g$ , and  $V_f(T)$  and  $V_f(T_g)$  are the fractional free volumes at  $T$  and  $T_g$ , respectively. Without regard to physical interpretation one can use, as an empirical result from Simha-Boyer (52, 54), the relationship

$$\Delta\alpha = 0.113/T_g \quad (5)$$

It follows from Eqs. (3)-(5), and substitution of  $T_{\ell\ell}$  for  $T$  that

$$V_f(T_{\ell\ell}) = V_f(T_g) + 0.113(K_4 - 1) \quad (6)$$

To the extent that  $V_f(T_g)$  is constant, i.e., that  $T_g$  is indeed an iso-free volume state either from polymer to polymer, or as a function of molecular weight, it follows that  $T_{\ell\ell}$  is an iso-free volume state. If  $V_f(T_g)$  is given the Simha-Boyer value of 0.113, then, from Eq. (4)

$$V_f(T_{\ell\ell}) = \Delta\alpha T_{\ell\ell} \quad (7)$$

Thus, the free volume at  $T_{\ell\ell}$  is about 20% greater than that at  $T_g$ .

It has been noted (5) that the shape of the TBA  $T_{\ell\ell}$  - log molecular weight plot for polymers with narrow distributions of molecular weight ( $M \lesssim M_c$ ) closely resembled an isoviscosity plot prepared by Hyun and Boyer (55) from zero shear melt viscosity,  $\eta_0$ , data as a function of temperature and molecular weight on polystyrene fractions. Figure 25 presents a similar isoviscosity plot of temperatures and molecular weights for which a series of anionic polystyrenes have a value of  $\eta_0 = 10^5$  poise. This was constructed from data reported by Plazek and O'Rourke (31). Also shown in Figure 25 are values of  $T_{\ell\ell}$  measured by the TBA method (Table VI of reference 5). It is seen that the two sets of data are again similar. Had  $\eta_0$  been selected as  $10^4$  poise all data points from reference 31 would lie above the TBA points.  $\eta_0 \approx 10^{4.5}$  poise would lead to very close coincidence of the two sets of data.

Melt viscosity at zero shear rate normally depends on  $\bar{M}_w$ , but for the anionic "monodisperse" polystyrenes  $\bar{M}_n \approx \bar{M}_w$  and hence there is no conflict between an iso free volume basis and an iso viscosity basis for the behavior

of  $T_{\ell\ell}$  vs. molecular weight for monodisperse specimens ( $M < M_c$ ).

In general,  $\bar{M}_w > \bar{M}_n$  and the problem of the isoviscosity state is more complicated. Simha (56) suggested that the general form of the melt viscosity equation (57) is:

$$\eta_o = F(T)\bar{M}_w^\beta$$

where  $F(T)$  would take the form of the Vogel equation, or equivalently, the WLF equation (58):

$$F(T) = A \exp[-E_o/R(T-T_o)]$$

where  $A$  and  $T_o$  are constants,  $E_o$  is an apparent activation energy and  $R$  is the gas constant. If  $\bar{M}_w > M_c$ ,  $\beta = 3.4$ , whereas if  $\bar{M}_w < M_c$ ,  $\beta = 1$ . If  $T = T_{\ell\ell} = F(\bar{M}_n)$  inspection of the melt viscosity equation shows that at low molecular weight the  $\bar{M}_n$  term will dominate, at high molecular weight the  $\bar{M}_w$  term will dominate and that at intermediate molecular weights both  $\bar{M}_n$  and  $\bar{M}_w$  are needed to characterize the viscosity.

The TBA  $T_{\ell\ell}$  relaxation for binary blends of low molecular weight polystyrenes ( $M_{A,B} < M_c$ ) has been shown (Figure 7) to average according to  $\bar{M}_n$  (6) and may therefore then represent an isoviscous state. However the TBA  $T_{\ell\ell}$  values for blends having at least one component with  $M > M_c$  do not represent isoviscosity states since unlike viscosity the temperature location of  $T_{\ell\ell}$  does not depend on the proportional amount of the lower molecular weight component (2, 6).

ACKNOWLEDGMENT: Partial support by the Chemistry Branch of the Office of Naval Research is acknowledged.

#### REFERENCES

1. R. F. Boyer, Rubber Chem. Tech., 36, 1303 (1963).
2. E. A. Sidorovich, A. I. Marei and N. S. Gashtol'd, Rubber Chem. Tech., 44, 166 (1971).
3. F. Ueberreiter and J. Naghizadeh, Kolloid Z.Z. Polym., 250, 927 (1972).
4. L. A. Utracki, J. Macromol. Sci., Phys., B-10, 477 (1974).
5. S. J. Stadnicki, J. K. Gillham and R. F. Boyer, J. Appl. Polym. Sci., 20 (5), 1245 (1976).
6. C. A. Glandt, H. K. Toh, J. K. Gillham and R. F. Boyer, J. Appl. Polym. Sci., 20 (5), 1277 (1976). See ibid, 20 (7), 2009 (1976).
7. J. K. Gillham, J. A. Benci and R. F. Boyer, Polym. Eng. Sci., 16 (5), 357 (1976).
8. J. K. Gillham and R. F. Boyer, Amer. Chem. Soc., Polym. Prepr., 17 (2), 171 (1976).
9. R. F. Boyer, Polymer, 17 (11), 996 (1976).
10. R. F. Boyer and J. K. Gillham, Amer. Chem. Soc., Polym. Prepr., 18 (1) 623 (1977).
11. R. F. Boyer and J. K. Gillham, Polymer, submitted manuscript (1976).  
 A manuscript submitted to Polymer has been withdrawn in order to include its essential contents in the present paper under the heading of:  
 Title: An Iso-Free Volume State.
12. J. B. Enns, R. F. Boyer and J. K. Gillham, Polymer, submitted manuscript.
13. J. B. Enns and R. F. Boyer, Amer. Chem. Soc., Polym. Prepr., 18 (1), 629 (1977).
14. J. K. Gillham, A.I.Ch.E. Journal, 20 (6), 1066 (1974).
15. J. K. Gillham, S. J. Stadnicki and Y. Hazony, J. Appl. Polym. Sci., 21 (2), 401 (1977).
16. Calculations performed for the authors by Y. Hazony, Princeton University, June 1975.

17. W. P. Cox, R. A. Isaaksen and E. H. Merz, J. Polym. Sci., 44, 149 (1960).
18. M. C. Shen and A. V. Tobolsky, "Plasticizer and Plasticizer Processes", Adv. in Chem. Series, Amer. Chem. Soc., No. 48, 27 (1965).
19. W. P. Cox, L. E. Nielsen and R. Keeney, J. Polym. Sci., 26, 365 (1957).
20. A. F. Burmester, The Dow Chemical Co., Midland, MI. An anionic PS,  $\bar{M}_n = 37,000$  was used to impregnate a stainless steel mesh cut into a 1/4 inch wide strip on the bias at 45°. This impregnated strip was tested in tension on the Rheovibron.
21. S. Onogi, H. Kato, S. Ueki and T. Ibaragi, J. Poly. Sci.: Part C 15, 481 (1966).
22. S. Onogi, T. Masuda and K. Kitagawa, Macromolecules 3, 109 (1970).
23. T. Masuda, K. Kitagawa, T. Inoue and S. Onogi, Macromolecules 3, 116 (1970).
24. J. D. Ferry, Viscoelastic Properties of Polymers, Wiley, New York, p. 424 ff., 1971.
25. G. W. West, R. N. Haward and B. Wright in "Advances in Polymer Science and Technology", S.C.I. Monograph No. 26, p. 348 (1967).
26. H. J. Karam, K. S. Hyun and J. C. Bellinger, Trans. Soc. Rheol. 13, 209 (1969).
27. R. S. Spencer and R. E. Dillon, J. Colloid Sci., 4, 241 (1949).
28. W. J. Schell, R. Simha, and J. J. Aklonis, J. Macromol. Sci. Chemistry A-3, 1297 (1969).
29. K. S. Hyun, Polym. Eng. Sci. 14, 666 (1974).
30. K. S. Hyun and R. F. Boyer, "Ency. Poly. Sci. Tech.", Wiley, Interscience, New York, Vol. 13, 357 (1970).
31. D. J. Plazek and V. M. O'Rourke, J. Poly. Sci., A-2, 9, 1209 (1971).
32. K. Ueberreiter, "Plasticization and Plasticizer Processes", Amer. Chem. Soc., Advances in Chemistry Series, No. 48, Ch. 3 (1975).
33. K. Ueberreiter and H-J. Orthmann, Kunststoffe, 48, 525 (1958).

34. C. I. Chung and J. G. Gale, J. Poly. Sci. Polym. Phys., 14, 1149 (1976).
35. P. F. Erhardt, J. J. O'Malley and R. G. Crystal, in "Block Copolymers" (ed. S. L. Aggarwal), Plenum, New York, p. 195 ff., 1970.
36. G. Kraus and K. W. Rollmann, J. Poly. Sci. Physics, 14, 1133 (1976).
37. W. Kauzmann, Chem. Rev., 43, 219 (1948).
38. N. Hirai and H. Eyring, J. Poly. Sci., 37, 51 (1959).
39. B. Wunderlich, J. Phys. Chem., 64, 1052 (1960).
40. J. M. O'Reilly and F. E. Karasz, J. Poly. Sci., C-14, 49 (1966).
41. P. Heydemann and H. D. Guicking, Kol. Z.Z. Polymere, 193, 16 (1964).
42. R. Simha, and R. A. Haldon, J. Appl. Phys., 39, 1890 (1968).
43. W. J. Schell, R. Simha, and J. J. Aklonis, J. Macromol. Sci. Chem., A3, 1297 (1969).
44. J. M. Roe, and R. Simha, Int. J. Polymeric Mater., 3, 193 (1974).
45. R. F. Boyer, in "Thermal Analyses," (ed. H. G. Wiedemann) Vol. 3, Proc. Third ICTA, Davos 1971, pages 3-18 (1972). Birkhauser Verlag, Basel and Stuttgart.
46. P. Ehrenfest, Commun. Kamerlingh Onnes Lab. Univ. Leiden Suppl. No. 75b, 1933. See also J.E. Mayer and S.F. Streeter, J. Chem. Phys., 7, 1019 (1939).
47. R. Rands, W. Ferguson and J. Prather, J. Res. Nat'l. Bur. Stds., 33, 63 (1944).
48. K. Ueberreiter, Kol. Z. Z. Polymere, 216/217 (1967).
49. J. L. Duda and J. S. Vrentas, J. Poly. Sci., A-2, 6, 675 (1968).
50. J. B. Enns and R. F. Boyer, Amer. Chem. Soc., Polymer Preprints, 18(2), 000 (1977).
51. G. D. Patterson, H. E. Bair and A. E. Tonelli, J. Poly. Sci. C-54, 249 (1976).
52. R. Simha and R. F. Boyer, J. Chem. Phys., 37, 1003 (1962).
53. M. L. Williams, R. F. Landel and J. D. Ferry, J. Am. Chem. Soc., 77, 3701 (1955).
54. R. F. Boyer and R. J. Simha, J. Poly. Sci., Polymer Letters, 11, 33 (1973).
55. K. S. Hyun and R. F. Boyer, in 'Ency. Polym. Sci. Tech.' ed. N. Bikales, Wiley-Interscience, NYC 1970, Vol. 13, 349ff, especially Fig. 15, p. 369.
56. Professor R. Simha, Case Western Reserve University, Cleveland, Ohio, Private Communication (1976).
57. G. C. Berry and T. G. Fox, Advances Polym. Sci., 5, 261 (1968).
58. M. C. Williams, R. F. Landel and J. D. Ferry, J. Amer. Chem. Soc., 77, 3701 (1955).

#### FIGURE CAPTIONS

Figure 1. Automated TBA torsional pendulum. An electrical signal is obtained using a light beam passing through a pair of polarizers, one of which oscillates with the specimen. The pendulum is aligned and oscillations are initiated by a dedicated analog computer. The latter also processes the damped sine waves to provide the relative rigidity and logarithmic decrement which are plotted versus temperature (or time) in immediate time on an XY plotter (14).

Figure 2. TBA Torsional Pendulum.

The major components consist of:

- 1) The torsional pendulum [enclosed in a cabinet, top right; cabinet door open, bottom left].
- 2) The analog computer for automatic control of the experiment and data reduction [top center]. A printer and digital panel meter provide numerical values of the temperature (mV) or lapsed time, logarithmic decrement and period (P, seconds) of each damped wave [top center]. A monitoring strip chart recorder provides a continuous record of the waves and temperature (mV) [below computer].
- 3) A temperature controller/programmer [above computer].
- 4) An XY plotter which plots, immediately after computation, the relative rigidity ( $1/P^2$ ) and logarithmic decrement versus temperature (mV) or log time [top left].

- 5) Various switches permit selection of options, such as on, off, or reverse of temperature programming at upper and lower set points, selection of temperature or time as the running variable, etc. [top center].
- 6) Specimens, such as braid and film. The film is shown assembled with lower and upper extension rods ready for lowering into the TBA apparatus. The polaroid disc transducer is also shown. [Bottom right].

Figure 3. TBA thermomechanical spectra [relative rigidity ( $1/P^2$ ) and logarithmic decrement ( $\Delta$ ) vs. temperature (mV, iron constantan thermocouple)] of a polystyrene (anionic,  $\bar{M}_n = 37,000$ ;  $\bar{M}_w/\bar{M}_n < 1.1$ ).

Figure 4. TBA mechanical loss versus temperature for polystyrene [anionic,  $\bar{M}_n = 10,300$ ,  $\bar{M}_w/\bar{M}_n = 1.12$ ]. Logarithmic decrement ( $\Delta$ ), exponential damping constant ( $\alpha$ ), and out-of-phase shear modulus ( $G''$ ) versus temperature. These plots were obtained from the raw digital print-out of the paper tape by transfer to an interacting computer facility which utilized a graphic extension of APL on a Tektronix 4013 display terminal (16). Numerical values for the ordinates are proportional to the absolute values for the composite specimen. We are grateful to Professor M. Szwarc, State University of New York, Syracuse, New York for providing the characterized sample of "monodisperse" polystyrene.

Figure 5. TBA and DTA. Anionic monodisperse polystyrenes:  $T_g$  and  $T_{22}$  vs.  $1/M$  (for DTA,  $T_g$  was defined as the peak of the endotherm) (5).

- Figure 6. TBA and DTA. Anionic monodisperse polystyrenes:  $T_g$ ,  $T_{min}$  and  $T_{\ell\ell}$  vs.  $\log M$  (5).
- Figure 7. TBA. Blends of monodisperse anionic polystyrenes ( $\bar{M}_n = 2,050$ ;  $\bar{M}_n = 20,200$ ): effect of  $\bar{M}_n$  on  $T_g$  and  $T_{\ell\ell}$  and of  $\bar{M}_w$  on  $T_{\ell\ell}$  (6).
- Figure 8. TBA. Thermomechanical spectra (logarithmic decrement vs. temperature) of a plasticized polystyrene: effect of composition (weight percent plasticizer/weight percent polystyrene) (7). Anionic polystyrene:  $\bar{M}_n = 37,000$ ;  $\bar{M}_w/\bar{M}_n < 1.1$ . Plasticizer:  $(C_6H_5OC_6H_4O)_2C_6H_4$ . Curves have been displaced vertically by arbitrary amounts for purposes of clarification.
- Figure 9. TBA. Plasticized polystyrene:  $T_g$ ,  $T_{min}$ ,  $T_{\ell\ell}$  and  $T_{\ell\ell}'$  vs. weight percentage of plasticizer<sup>(7)</sup>. Anionic polystyrene:  $\bar{M}_n = 37,000$ ;  $\bar{M}_w/\bar{M}_n < 1.1$ . Plasticizer:  $(C_6H_5OC_6H_4O)_2C_6H_4$ .
- Figure 10. TBA. Homopolymers, polystyrene/polystyrene blends and plasticized polystyrene:  $T_{\ell\ell}$ ,  $T_{\ell\ell}'$  and  $T_{min}$  ( $^{\circ}K$ ) vs.  $T_g$  ( $^{\circ}K$ ) (7).
- Figure 11. Schematic dynamic viscosity,  $\eta'$  vs.  $\omega$  plots copied from data of Cox et al. (19). The dashed lines represent our extrapolations. A cross-plot of  $\eta'$  vs. temperature at  $5 \text{ rad. sec}^{-1}$  is shown in the inset to Figure 12 (10).
- Figure 12. Inset.  $\eta'$  at  $5 \text{ rad. sec}^{-1}$  vs.  $T$  ( $^{\circ}C$ ) from cross-plot of Figure 11 (10). Main curves (left):  $\log \omega$  ( $\text{rad. sec}^{-1}$ ) vs.  $1/T_{\ell\ell}$  plot for 3 frequencies from Figure 11, providing an apparent activation energy for  $T_{\ell\ell}$  of  $30 \text{ Kcal mol}^{-1}$ ; (right):  $\log f$  (Hz) vs.  $1/T_g$  at  $\bar{M}_n = 37,000$  providing an apparent activation energy for  $T_g$  of  $130 \text{ Kcal mole}^{-1}$  [data from Ref. (20)].

- Figure 13. Inset. Dynamic melt viscosity ( $\eta'$ ) data of Onogi et al. (22) vs. molecular weight ( $\bar{M}_v$ ).  
Main curve. Low  $\omega$  vs.  $\log \bar{M}_v$  from maxima of plots in inset (10).
- Figure 14. Zero shear melt viscosity,  $\eta_0$ , from capillary rheometry vs.  $1/T(^{\circ}\text{K})$  for heterogeneous polystyrenes from West et al. (25) and Karam et al. (26) (10).
- Figure 15.  $T_{\ell\ell}$  vs.  $\log$  molecular weight. Comparison of assignments made by TBA and from melt rheology literature (10).  $\bar{M}_n$  and  $\bar{M}_w$  values for the same specimen are connected by dashed lines. Numbers refer to Table 3 (left column).
- Figure 16. Comparison of  $T_{\ell\ell}$  by TBA from Figure 6 with temperature of fusion,  $T_F$ , from Ueberreiter and Orthmann (33).
- Figure 17. TBA. SBS triblock copolymer. (Microstructure: cis-1,4 40%, trans-1,4 49%, 1,2 11%).
- Figure 18. TBA. SBS triblock copolymer. (Microstructure: cis-1,4 25%, trans-1,4 34%, 1,2 41%).
- Figure 19. Precision specific heat data on an unvulcanized poly(butadiene-co 22.6 wt. % styrene) elastomer showing the characteristic  $\Delta C_p$  at  $T_g$  and a third order  $T_{\ell\ell}$  transition at 275 $^{\circ}\text{K}$ . The inset shows 1 Hz torsion pendulum loss data on an unvulcanized SBR of similar styrene content. Figure from Ref. 45.
- Figure 20. DSC scans on anionic polystyrene ( $\bar{M}_n = 17,500$ ) first as a powder (A) and then as a fused film (B) (12). Heating rates were 40 $^{\circ}\text{C}/\text{min}$ ; range attenuation was 8.
- Figure 21. A, B, C, D, E, and F. DSC traces on fused anionic polystyrene films having the indicated molecular weights (12). Values of  $T_g$  and  $T_{\ell\ell}$  in  $^{\circ}\text{C}$  are indicated. Heating rates were 40 $^{\circ}\text{C}/\text{min}$ ; range attenuation was 4.

Figure 22.  $T_g$  and  $T_{ll}$  in °K as a function of molecular weight, based on data in Figure 21 collected in Table 4 (12). The solid lines indicate DTA and TBA data from Figure 6.

Figure 23.  $T_{ll}$  vs.  $T_g$  in °C for polymethylmethacrylate fractions by thermal diffusivity (3) and for anionic polystyrenes (5) and their blends (6) by DTA and TBA.

Figure 24.  $T_{ll}$  vs.  $T_g$  in °K for the polymers studied (13). The line has slope = 1.2. The inset is a schematic DSC trace, showing  $T_g$  and  $T_{ll}$ .

Figure 25. Anionic polystyrene:  $T_{ll}$  (°C) by TBA vs. molecular weight (5); also temperature (°C) at which zero shear melt viscosity =  $10^5$  poise (31) vs. molecular weight.

#### TABLE CAPTIONS

1.  $T_{ll}$ :  $\Delta$  versus  $G''$  Assignments.
2. TBA. Plasticized Polystyrene: Effect of Composition on  $T_g$ ,  $T_{min}$  and  $T_{ll}'$ .
3. Evidence for  $T_{ll}$  by Conventional Melt Rheology.
4. DSC.  $T_g$  and  $T_{ll}$  from Fused Films of Anionic Polystyrene.

TABLE 1.  $T_{\ell\ell}$ :  $\Delta$  Versus  $G''$  Assignments (10)

Polymer	Molecular Weight	$T_{\ell\ell}$		$\Delta T$ (°C)
		$\Delta^b$	$G''^c$	
Polystyrene	10,000 ( $\bar{M}_n$ )	131	127	4
Polymethylmethacrylate	25,000 ( $\bar{M}_n$ )	174	168	6
Polyvinylacetate	a	110	96	14

<sup>a</sup> unavailable but  $T_g = 44^\circ\text{C}$  (1 Hz)

<sup>b</sup> from direct recording TBA (14)

<sup>c</sup> computed from  $dG'/dT$  (15,16)

TABLE 2. TBA. Plasticized Polystyrene: Effect of Composition on  $T_g$ ,  $T_{min}$ ,  $T_{\ell\ell}$  and  $T_{\ell\ell}'$

Weight Fraction Plasticizer <sup>b</sup>	$T_g$ , °K (Hz)	$T_{min}$ , °K (Hz)	$T_{\ell\ell}$ , °K (Hz)	$T_{\ell\ell}'$ , °K (Hz)
1.0	254 (0.6)	262.5 (0.37)	271.5 (0.29)	287 (0.21)
0.9016	257.5 (0.6)	268 (0.31)	285 (0.24)	310 (0.19)
0.7997	262 (0.6)	274 (0.37)	295 (0.27)	327 (0.20)
0.7003	269 (0.6)	284 (0.36)	306 (0.27)	350 (0.19)
0.5998	278 (0.6)	292 (0.38)	319 (0.26)	370 (0.18)
0.4983	289.5 (0.6)	305.5 (0.34)	332 (0.26)	383 (0.19)
0.3993	303 (0.6)	319.5 (0.37)	348 (0.27)	407 (0.19)
0.3000	319.5 (0.5)	336.5 (0.34)	366 (0.26)	
0.2002	336 (0.5)	353.5 (0.36)	386 (0.28)	
0.1000	356.5 (0.5)	375.5 (0.36)	405 (0.27)	
0.0	380.5 (0.5)	396.5 (0.32)	422 (0.24)	

<sup>a</sup> anionic polystyrene:  $\bar{M}_n = 37,000$ ,  $\bar{M}_w/\bar{M}_n < 1.1$ .

<sup>b</sup> plasticizer:  $(C_6H_5OC_6H_4O)_2C_6H_4$ .

TABLE 3: Evidence for  $T_{\infty}$  by Conventional  
Melt Rheology (10)

Method	f	Molecular Weight	$T_{\infty}$	Author	Refs.
1. Dynamic Viscosity	1.88 <sup>a</sup>	240,000	167	Cox et al.	(19)
2. Dynamic Viscosity	1.88 <sup>a</sup>	950,000	200	Onogi et al.	(21)
3. Dynamic Viscosity	1.88 <sup>a</sup>	68,000	160	Onogi et al. Masuda et al.	(22) (23)
4. Capillary Rheometry	--- <sup>b</sup>	$\bar{M}_n = 40,700$ $M_w = 89,000$	168	West et al. <sup>d,e</sup>	(25)
5. Capillary Rheometry	--- <sup>b</sup>	$\bar{M}_n = 107,000$ $M_w = 250,000$	180	Hyun	(29)
6. Capillary Rheometry	--- <sup>b</sup>	390,000	192	Spencer & Dillon <sup>d</sup>	(27)
7. Capillary Rheometry	--- <sup>b</sup>	$\bar{M}_n = 166,000$ $M_w = 355,000$	180	Karam et al. <sup>d,e</sup>	(26)
8. Rheovibron	3.5 <sup>c</sup>	$\bar{M}_n = 47,000$ <sup>f</sup>	165	Erhardt et al.	(35)

<sup>a</sup> radians sec<sup>-1</sup>  $\approx$  0.3 Hz (of TBA experiment)

<sup>b</sup> based on plots of  $\log \eta_0 - 1/T$  where the zero shear viscosity was extrapolated from finite shear rates

<sup>c</sup> Hz

<sup>d</sup> plots of  $\log \eta_0 - 1/T$  for these three sets of data are shown without experimental points as Figure 8, p. 357 of Ref. (30)

<sup>e</sup> data plotted in Fig. 14

<sup>f</sup> block copolymer of EO-PS,  $\bar{M}_n$  refers to PS block.

TABLE 4. DSC.  $T_g$  and  $T_{\ell\ell}$  from Fused Films of Anionic Polystyrenes  
(Heating at 40°C/min) (12)

$\bar{M}_n$ <sup>a</sup>	$\bar{M}_w/\bar{M}_n$ <sup>a</sup>	$T_g$ <sup>b</sup>	$T_{\ell\ell}$ <sup>b</sup>	$T_{\ell\ell}/T_g$ (°K/°K) <sup>c</sup>
2,200	1.10	47°C (320°K)	96°C (369°K)	1.15
4,000	1.10	68°C (341°K)	127°C (400°K)	1.17
17,500	1.06	87°C (360°K)	148°C (421°K)	1.17
37,000	1.06	95°C (368°K)	151°C (424°K)	1.15
110,000	1.06	98°C (371°K)	157°C (430°K)	1.16
2,000,000	1.30	103°C (376°K)	162°C (435°K)	1.16
			Av.	1.16

<sup>a</sup> data supplied by Pressure Chemical Co. , Pittsburgh, Pa.

<sup>b</sup> see figures 20 and 21 for definitions.

<sup>c</sup> a similar ratio is typical of torsional braid analysis. <sup>5,6,7</sup>

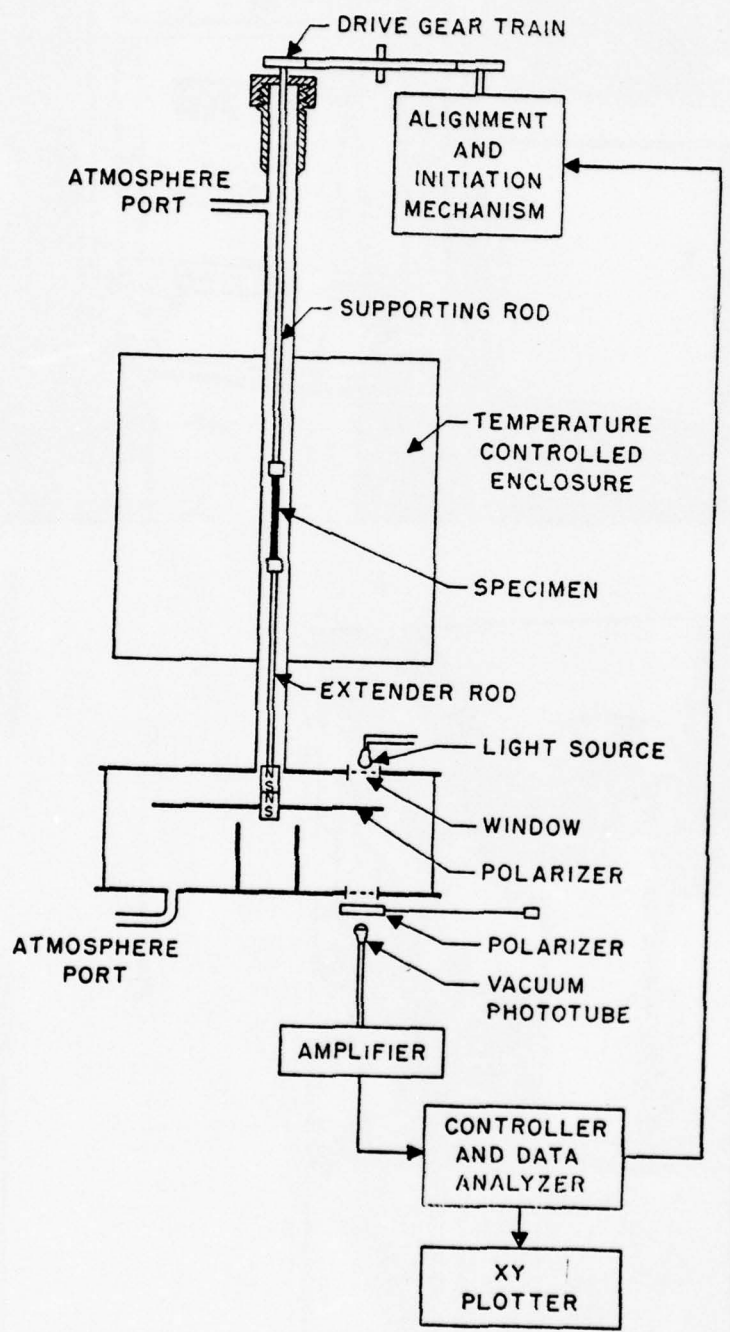


Figure 1

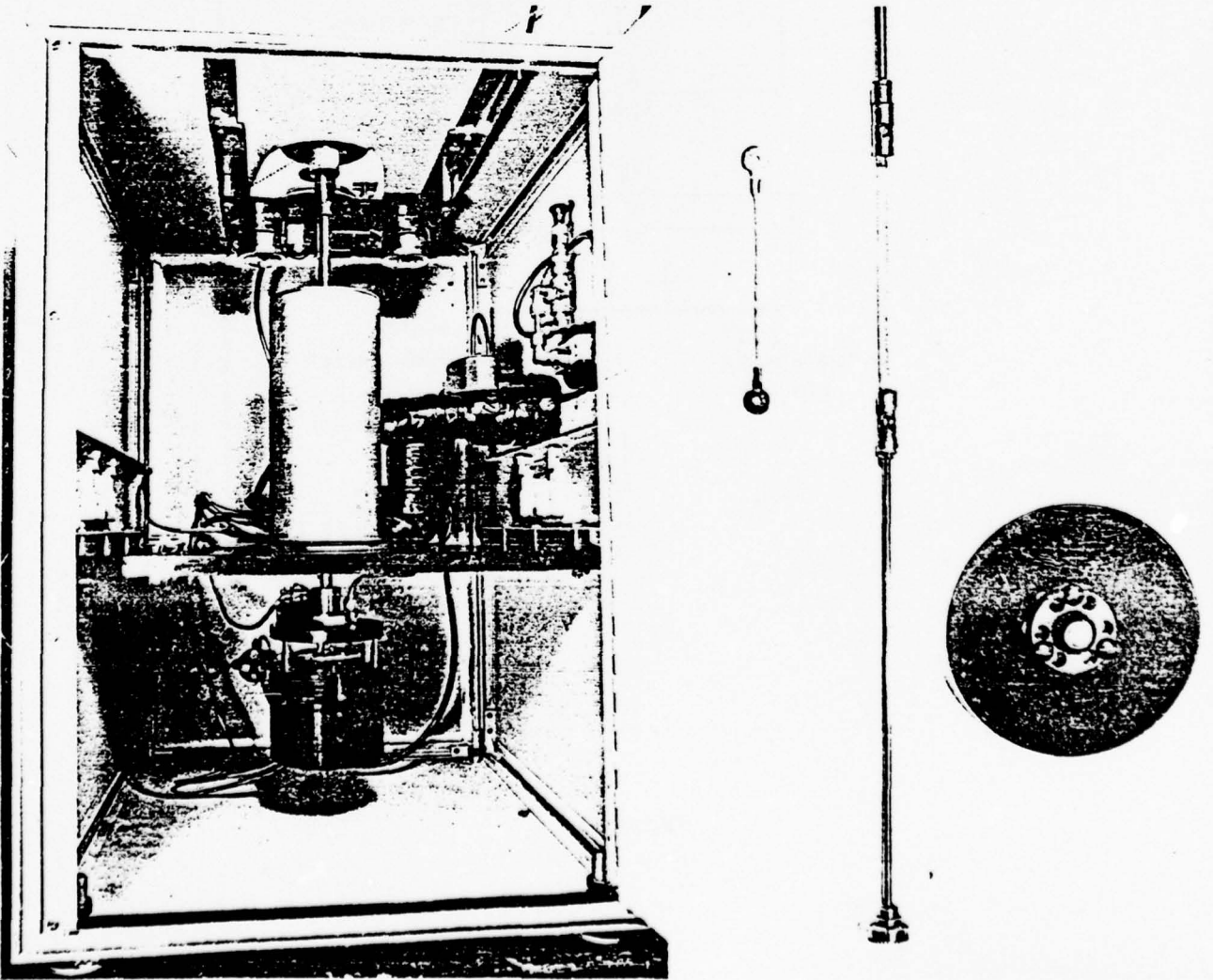
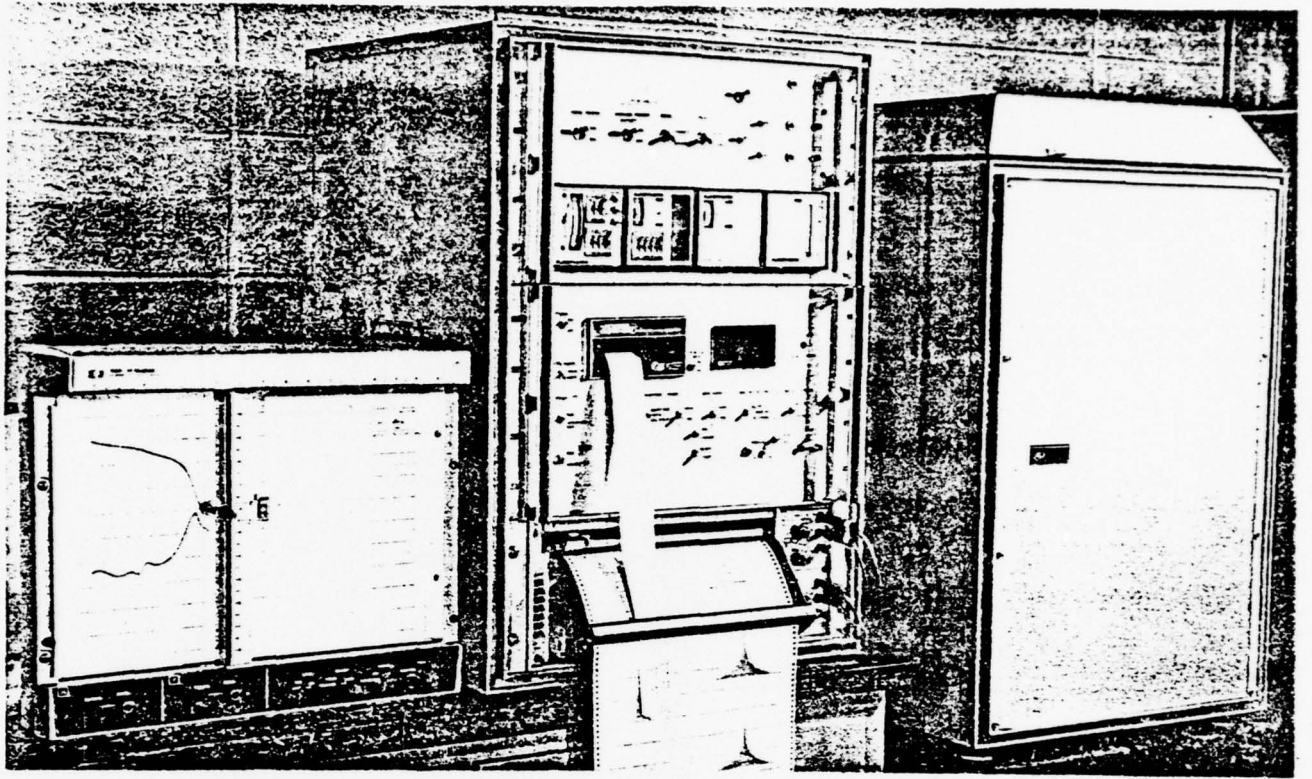


Fig. 2

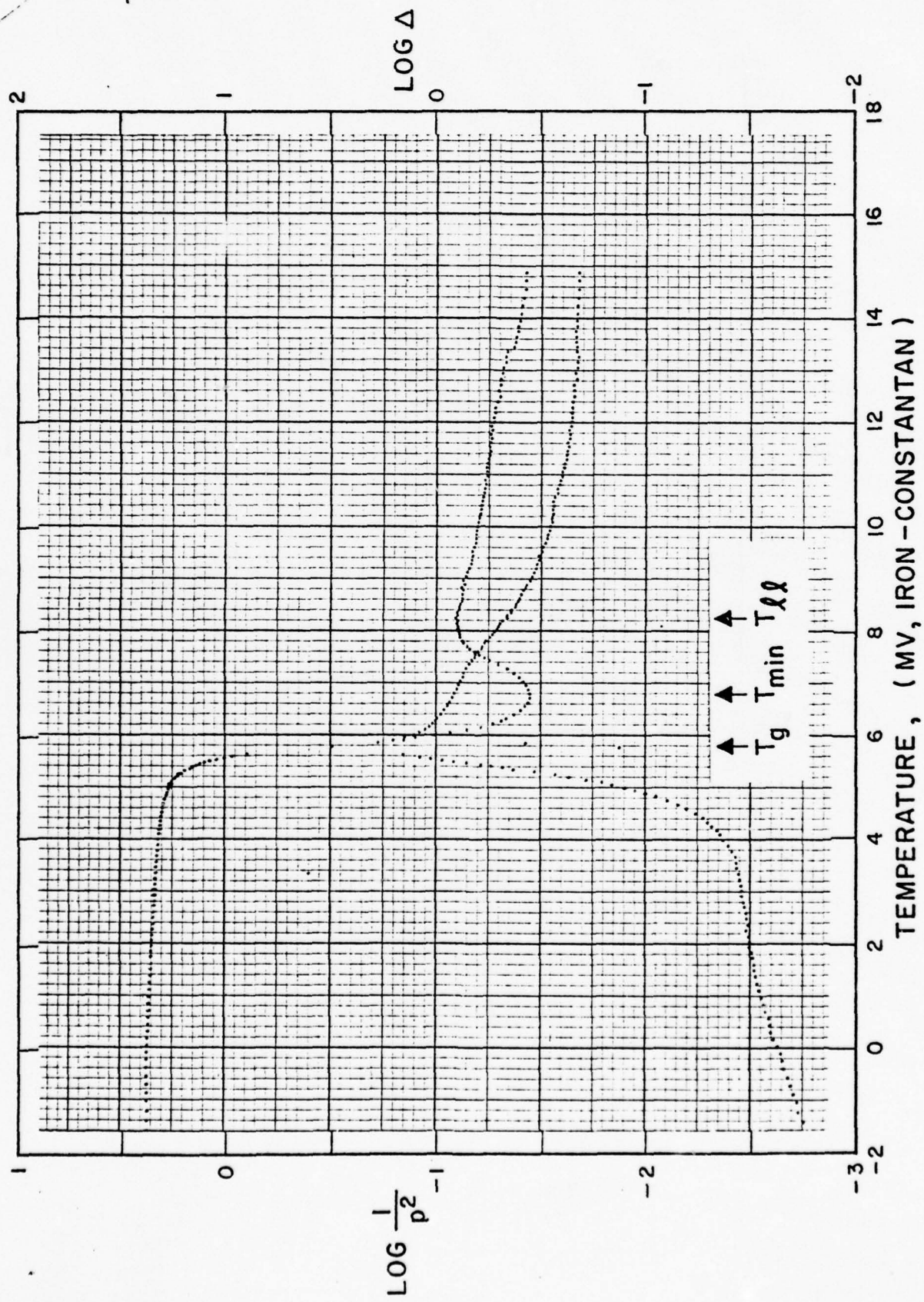


Fig. 3

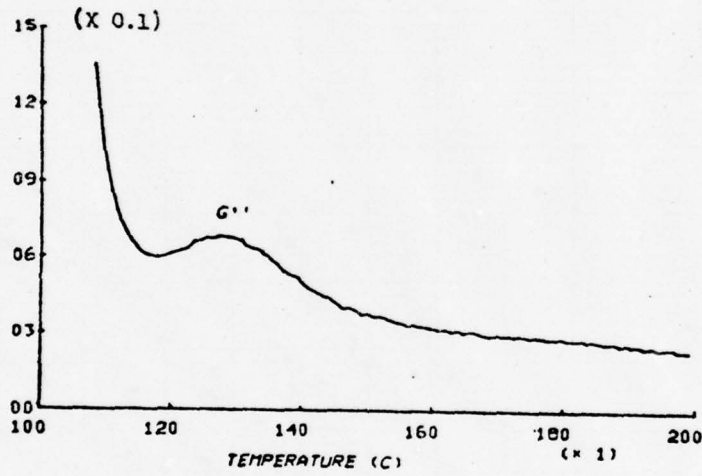
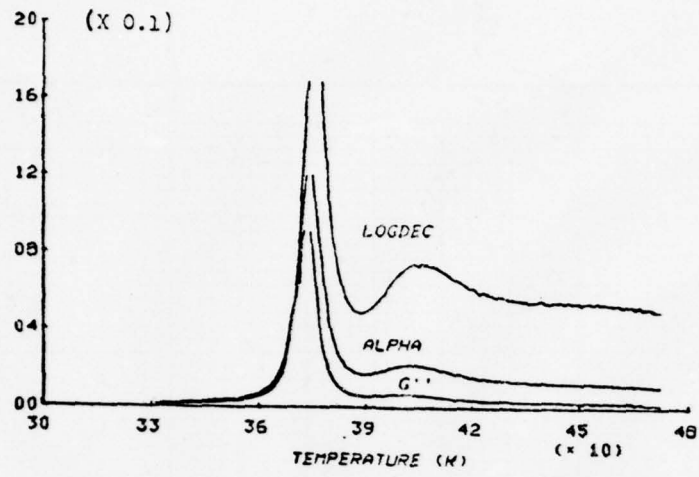


Fig. 4

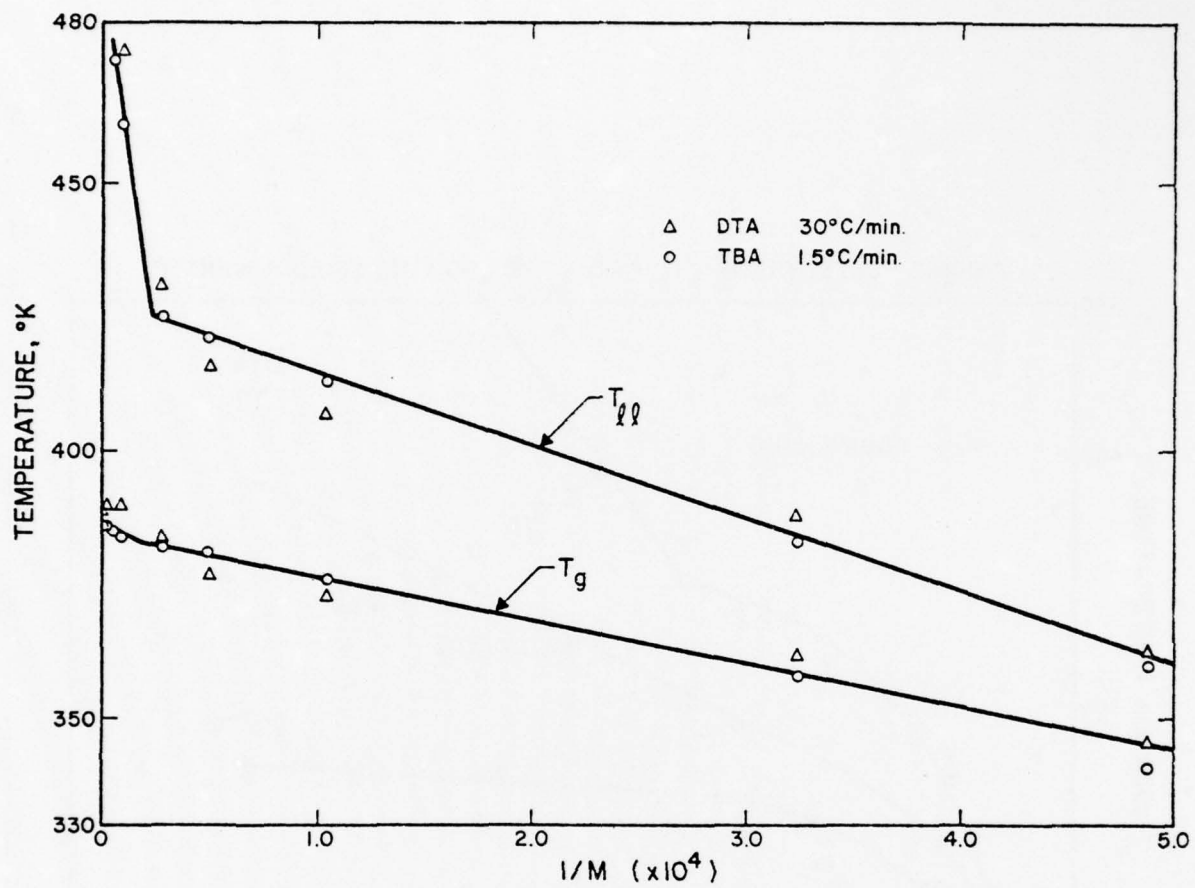


Figure 5

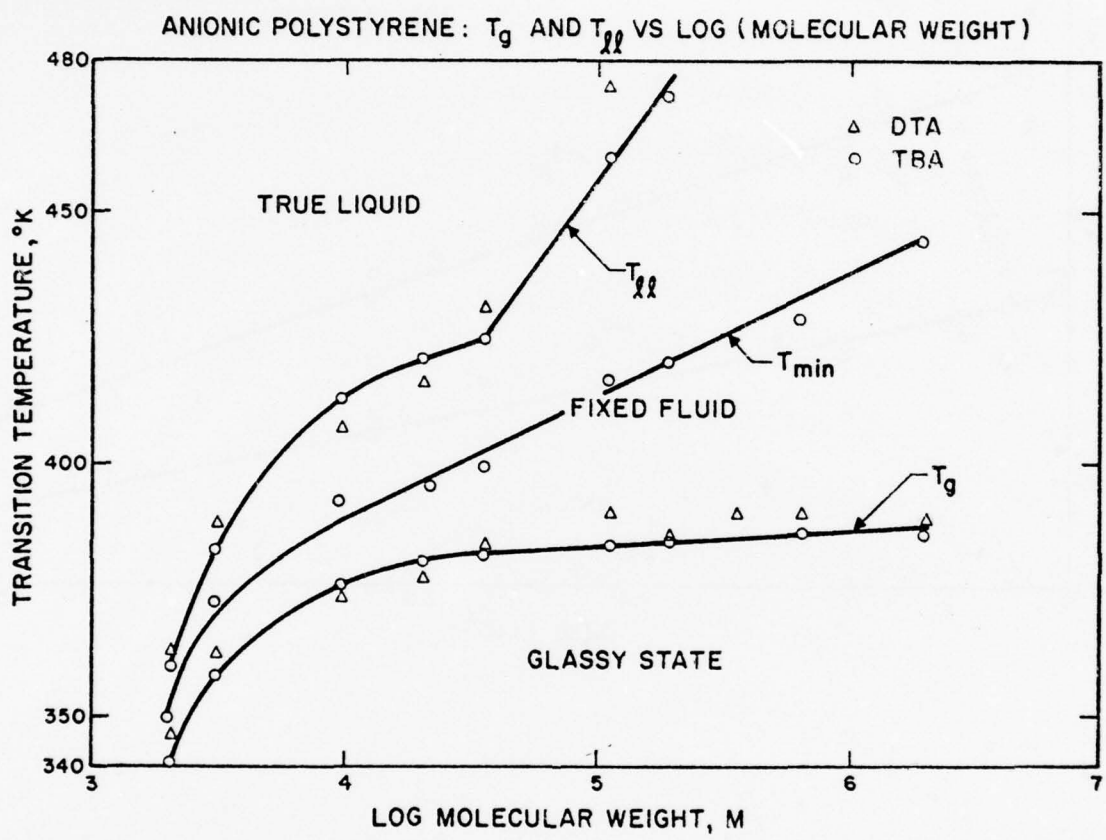


Figure 6

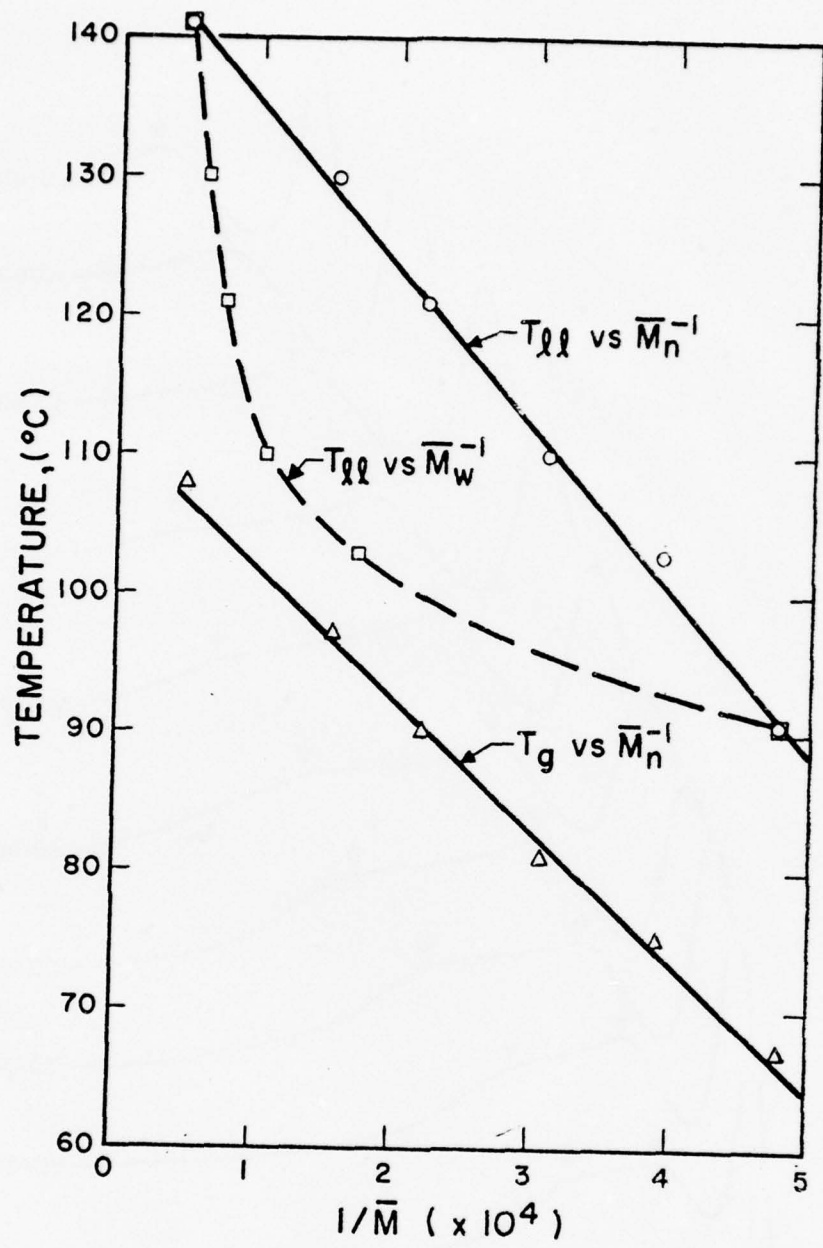


Figure 7

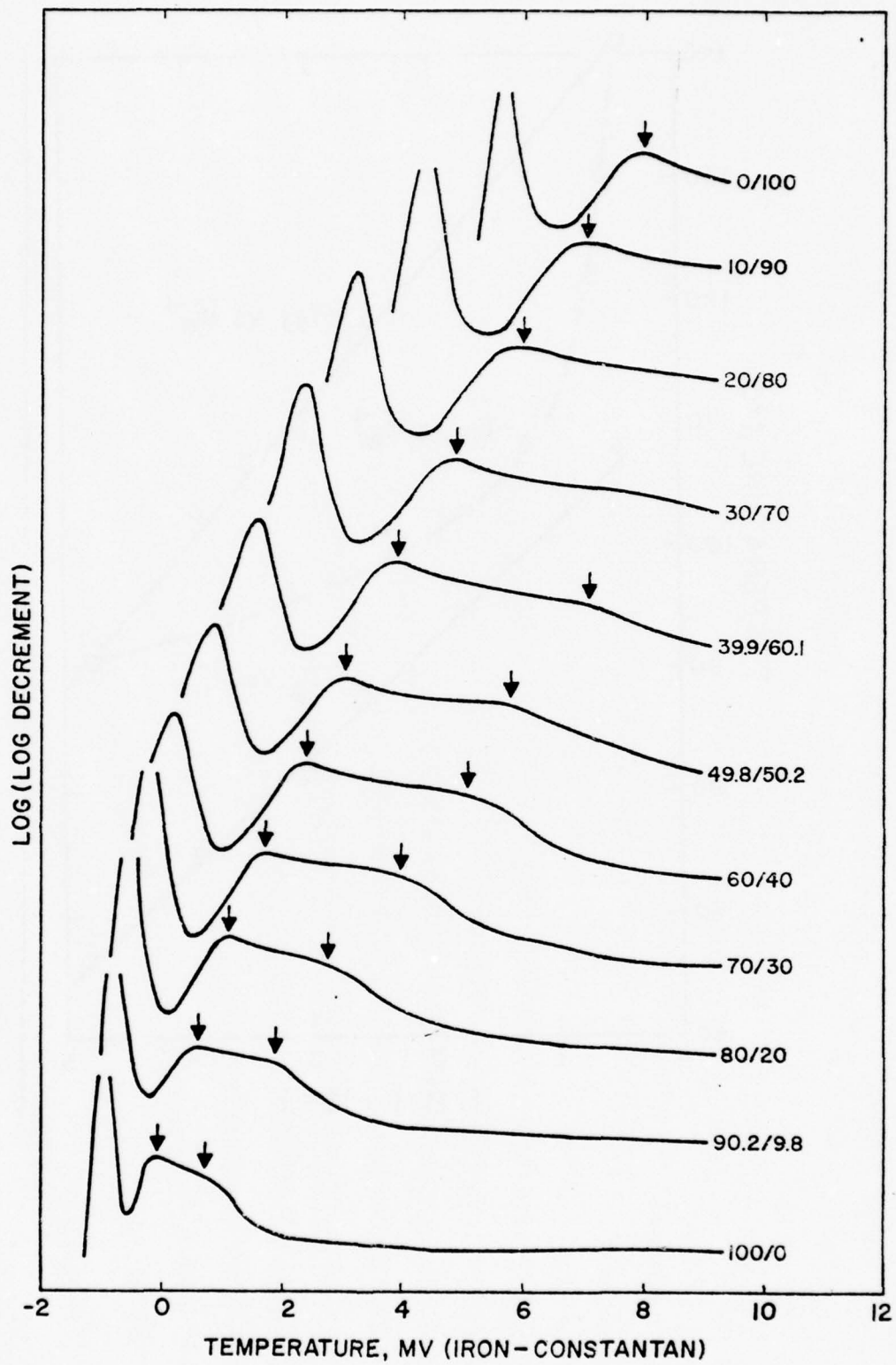


Figure 8

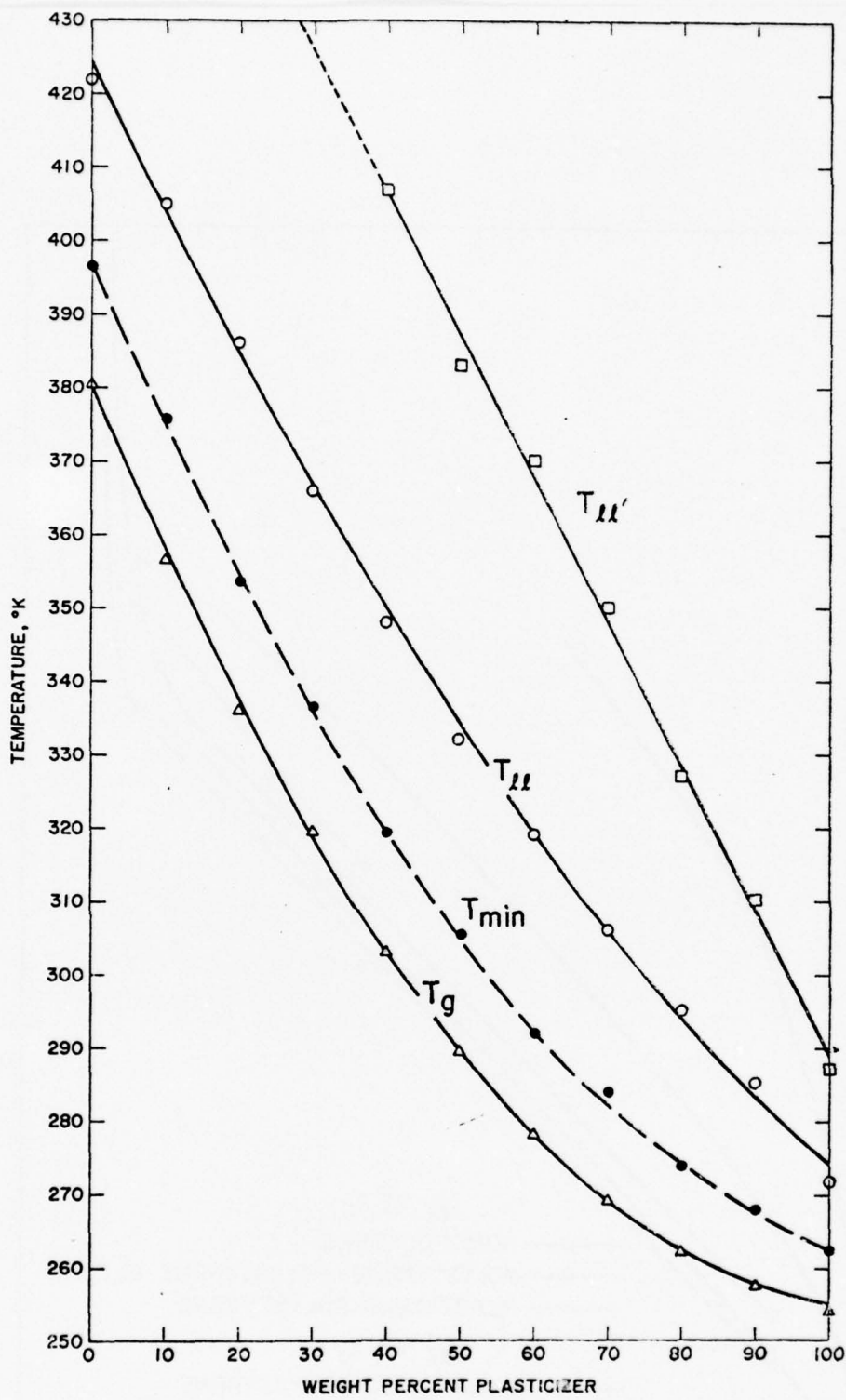


Figure 9

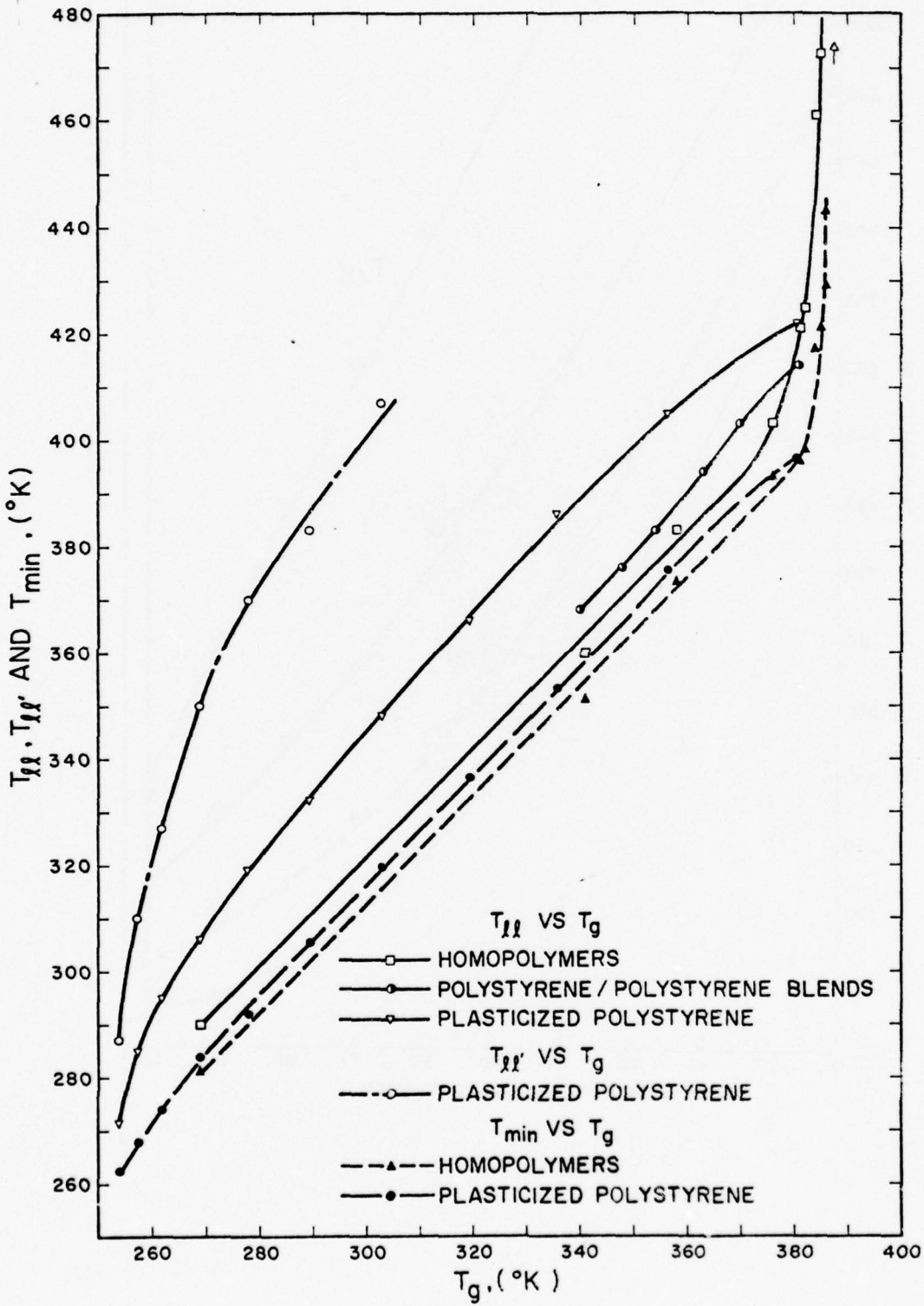


Fig. 10

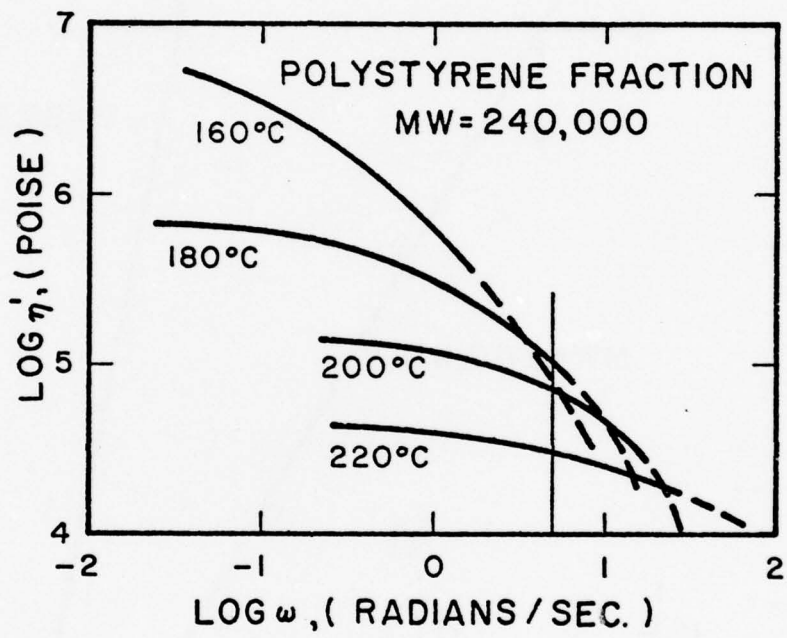


Fig. 11

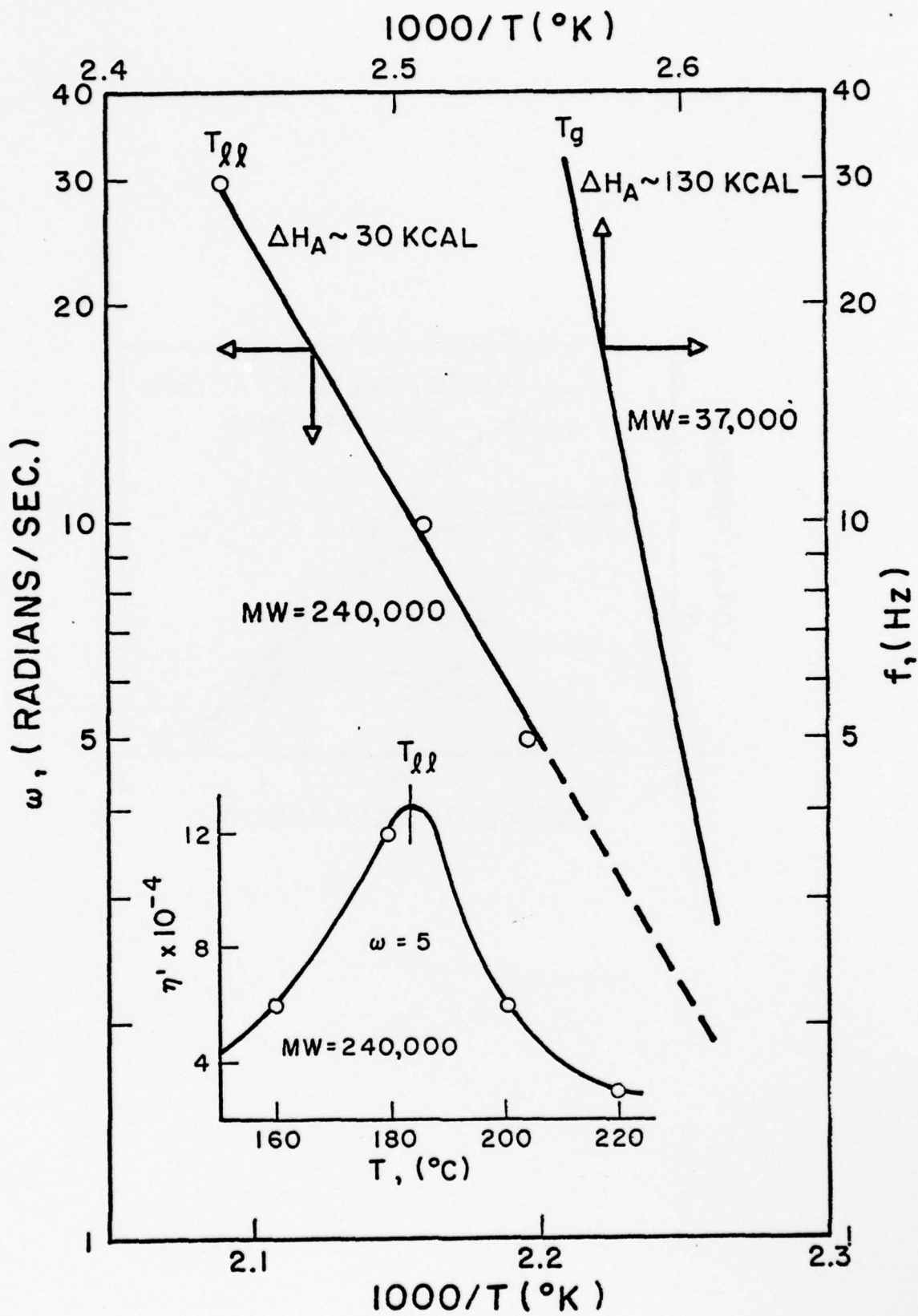


Fig. 12

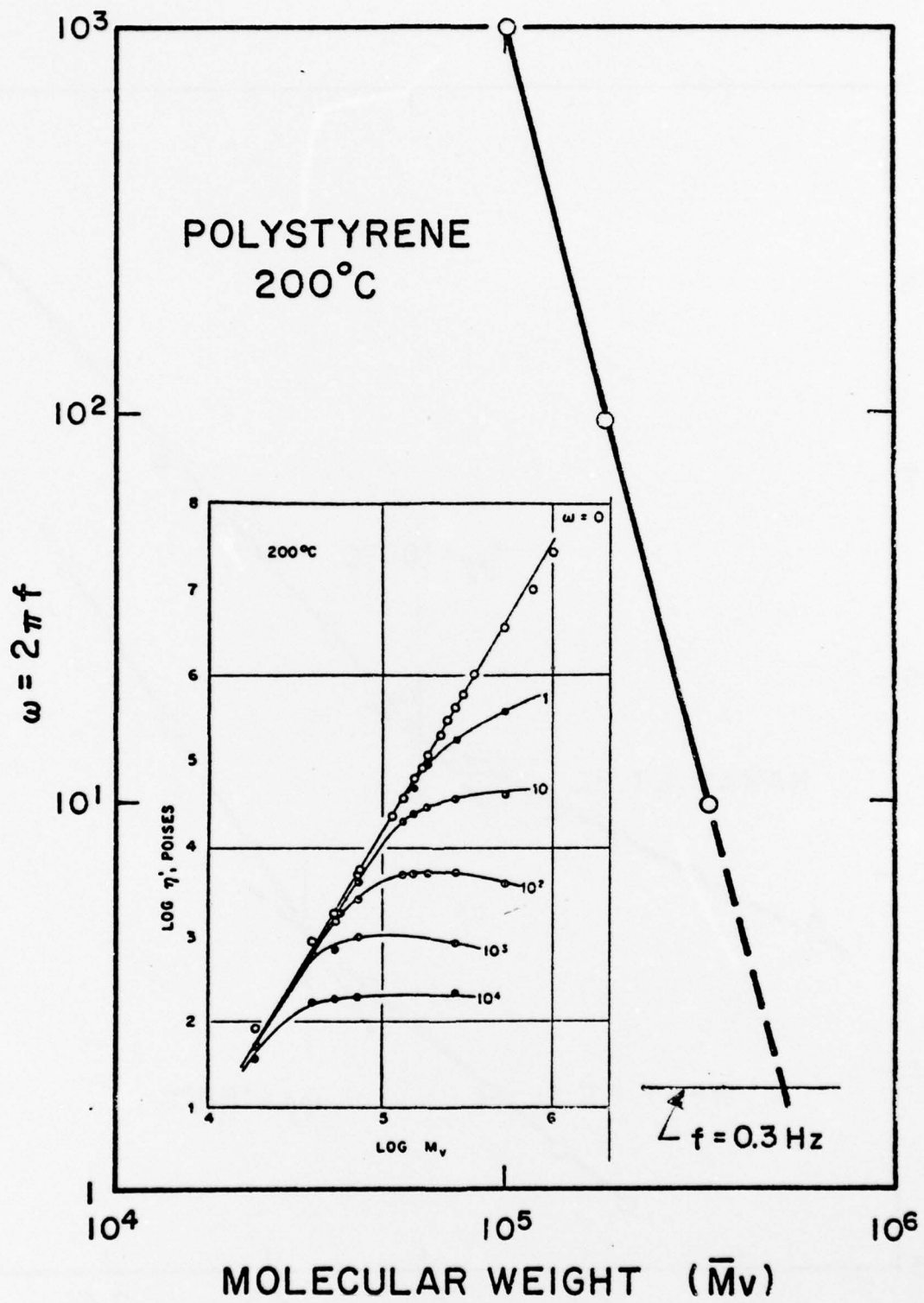


Fig. 13

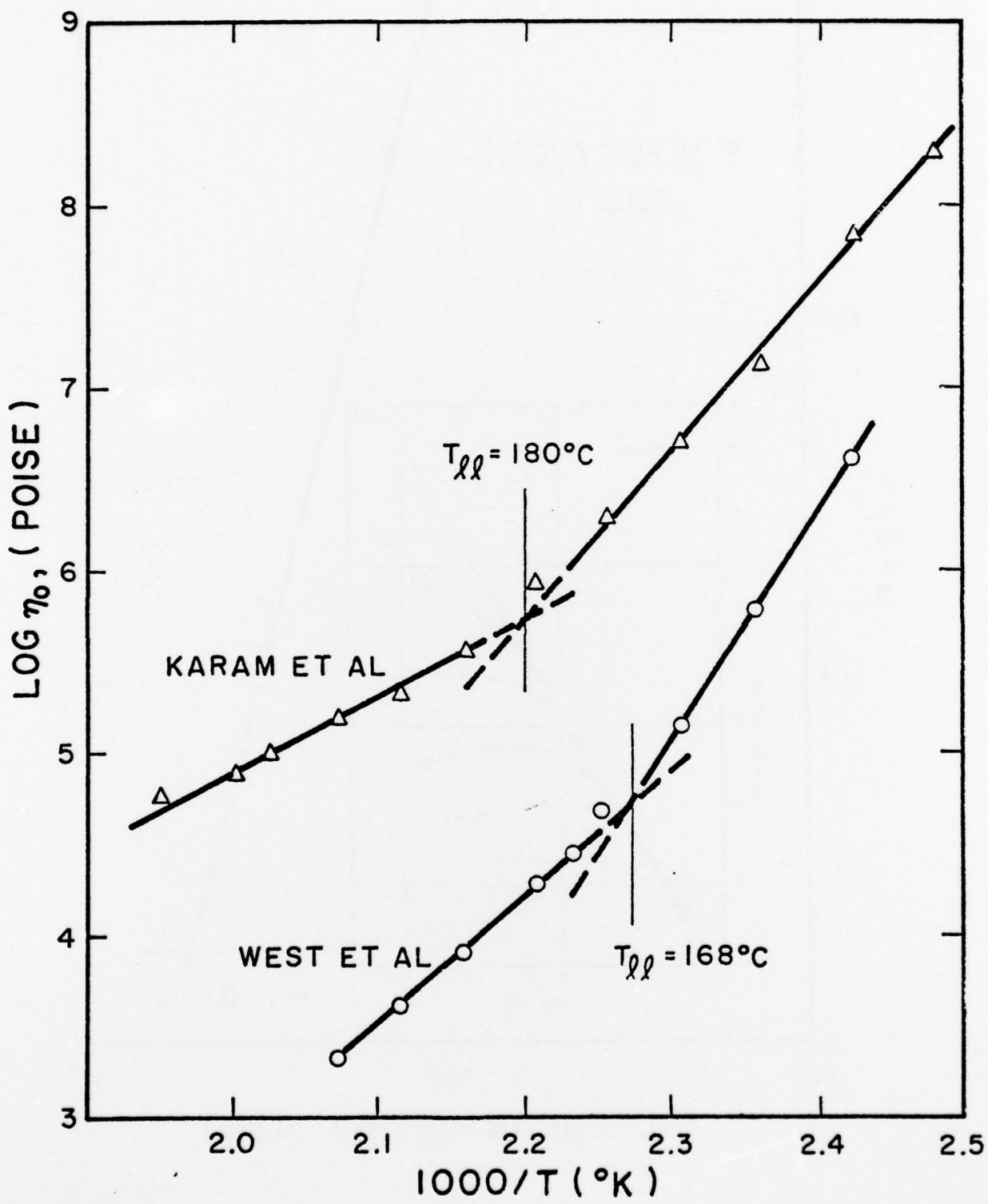


Fig. 14

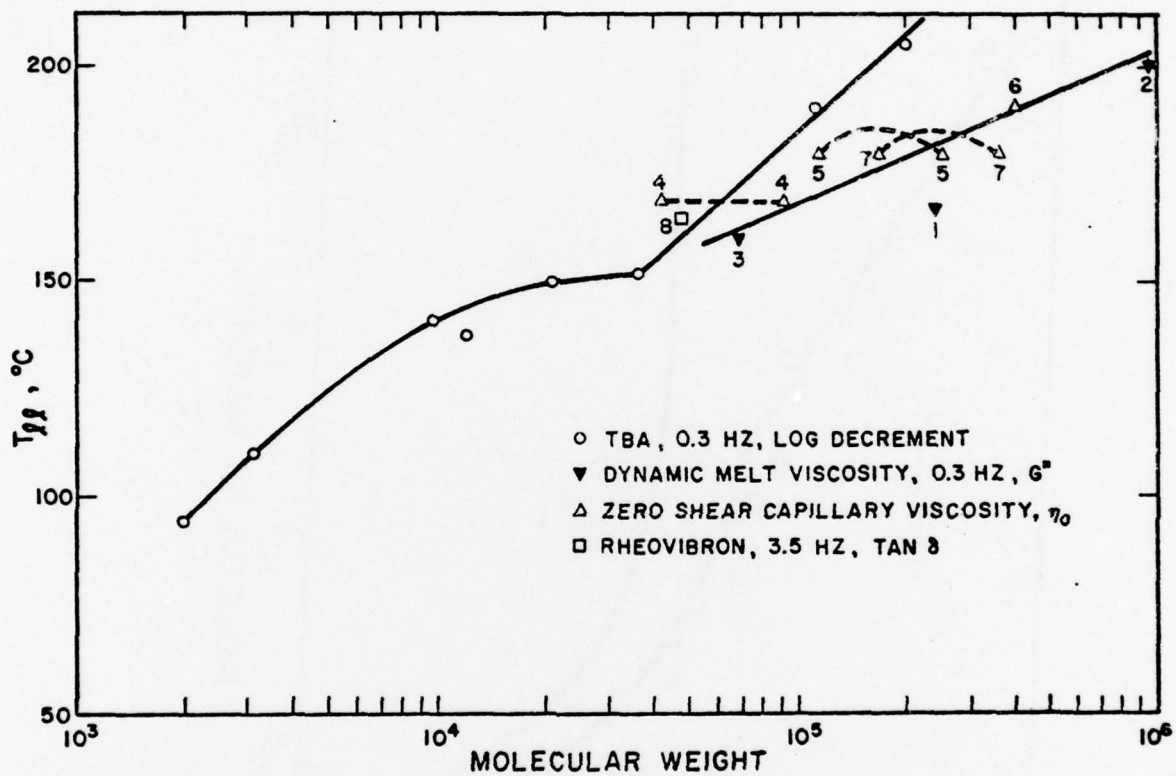


Figure 15

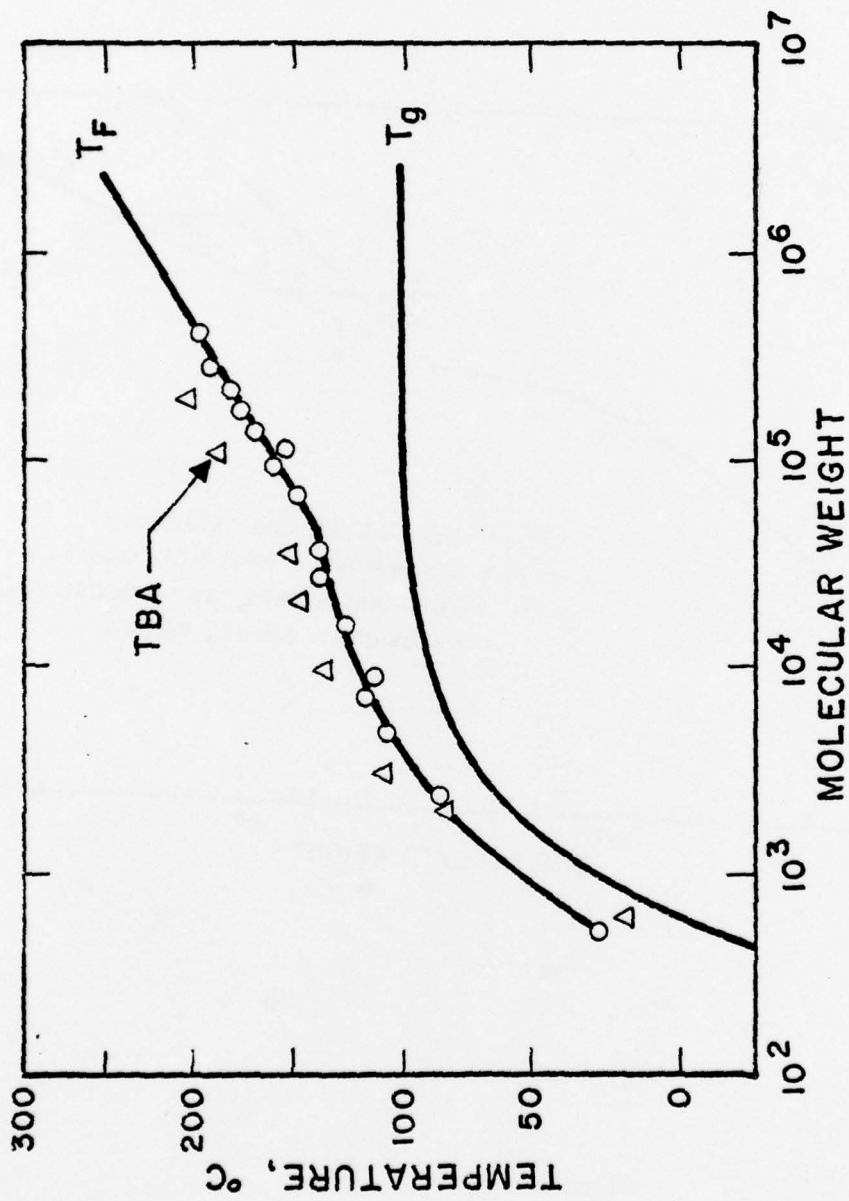


Fig. 16

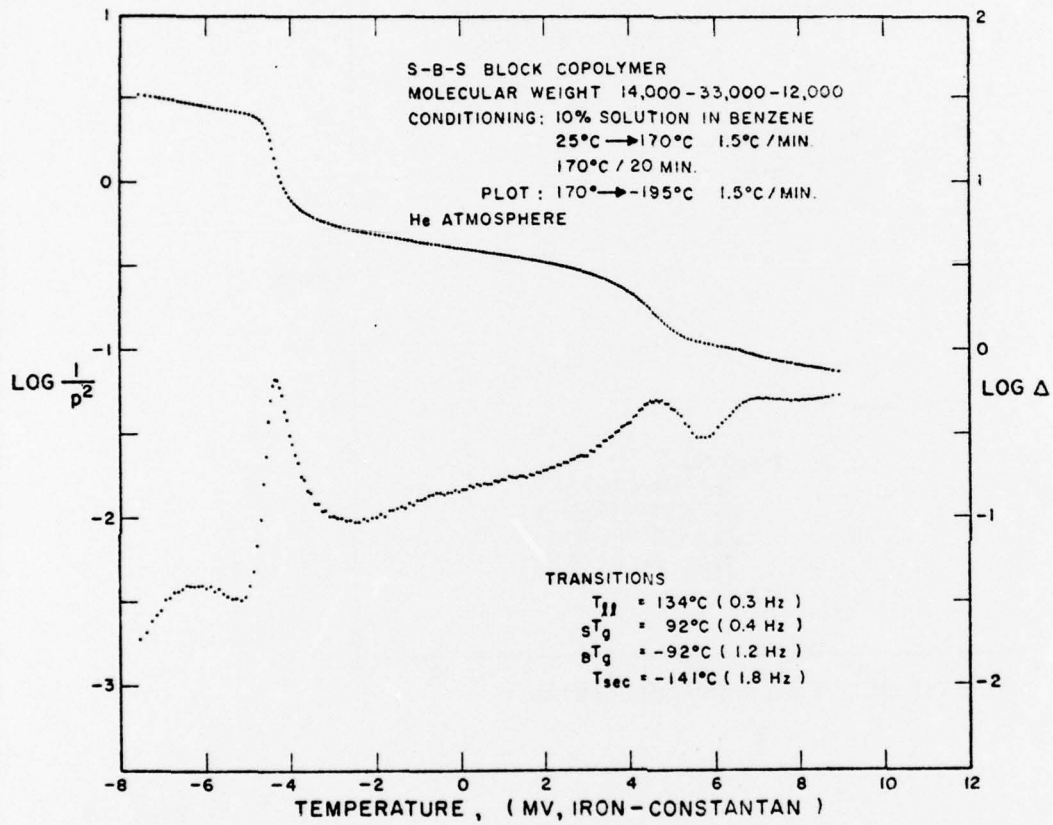


Fig. 17

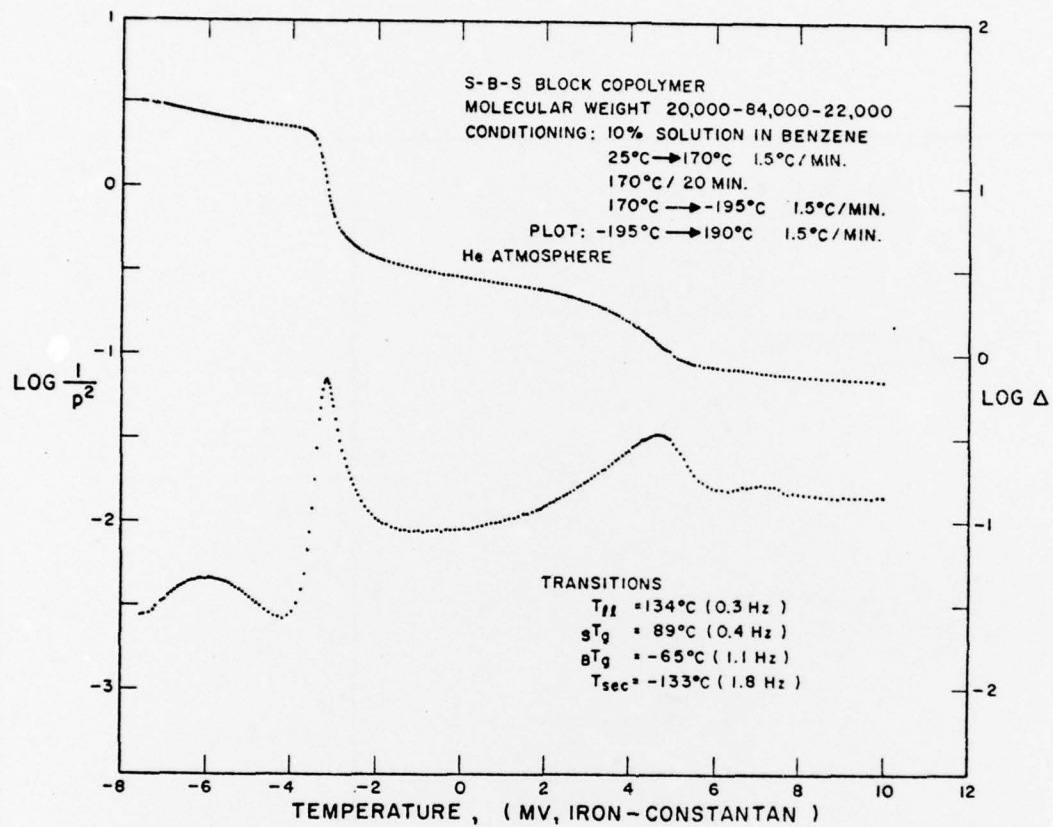


Fig. 18

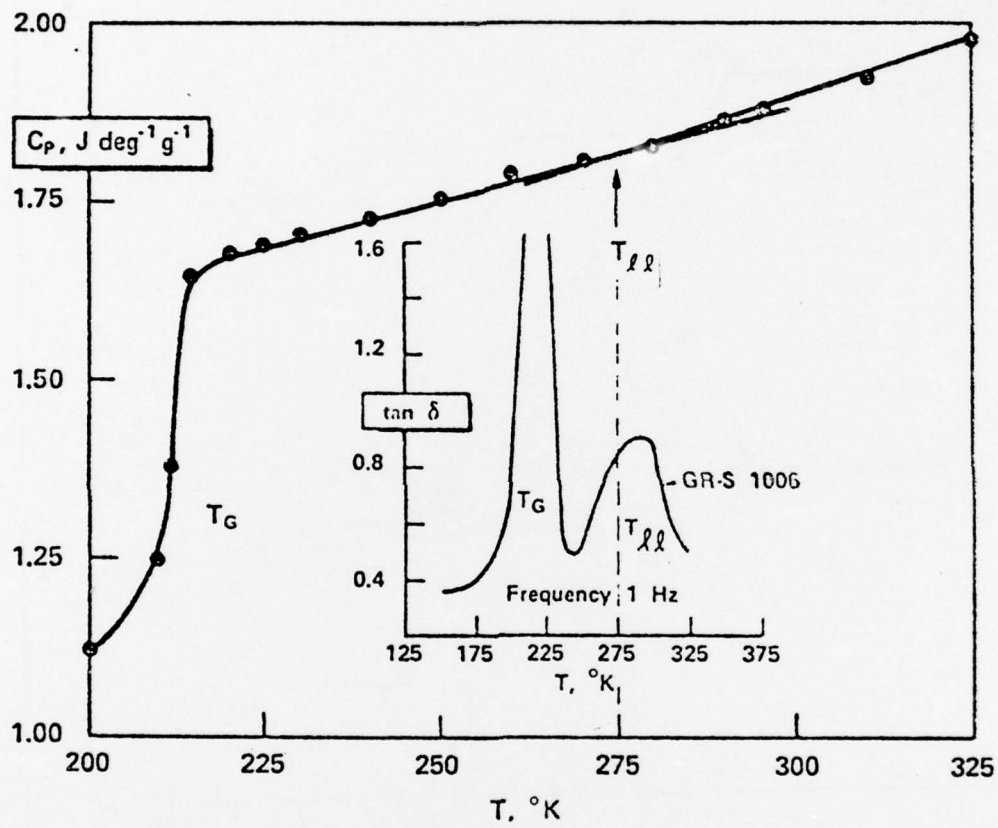


Fig. 19

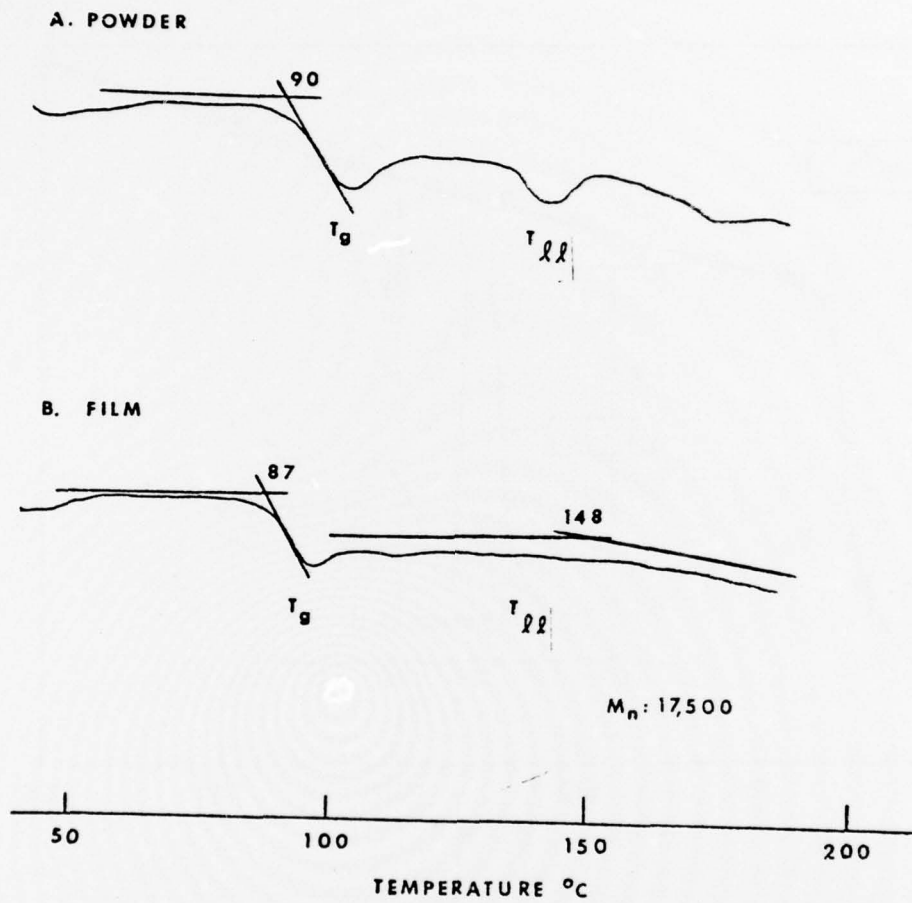


Fig. 20

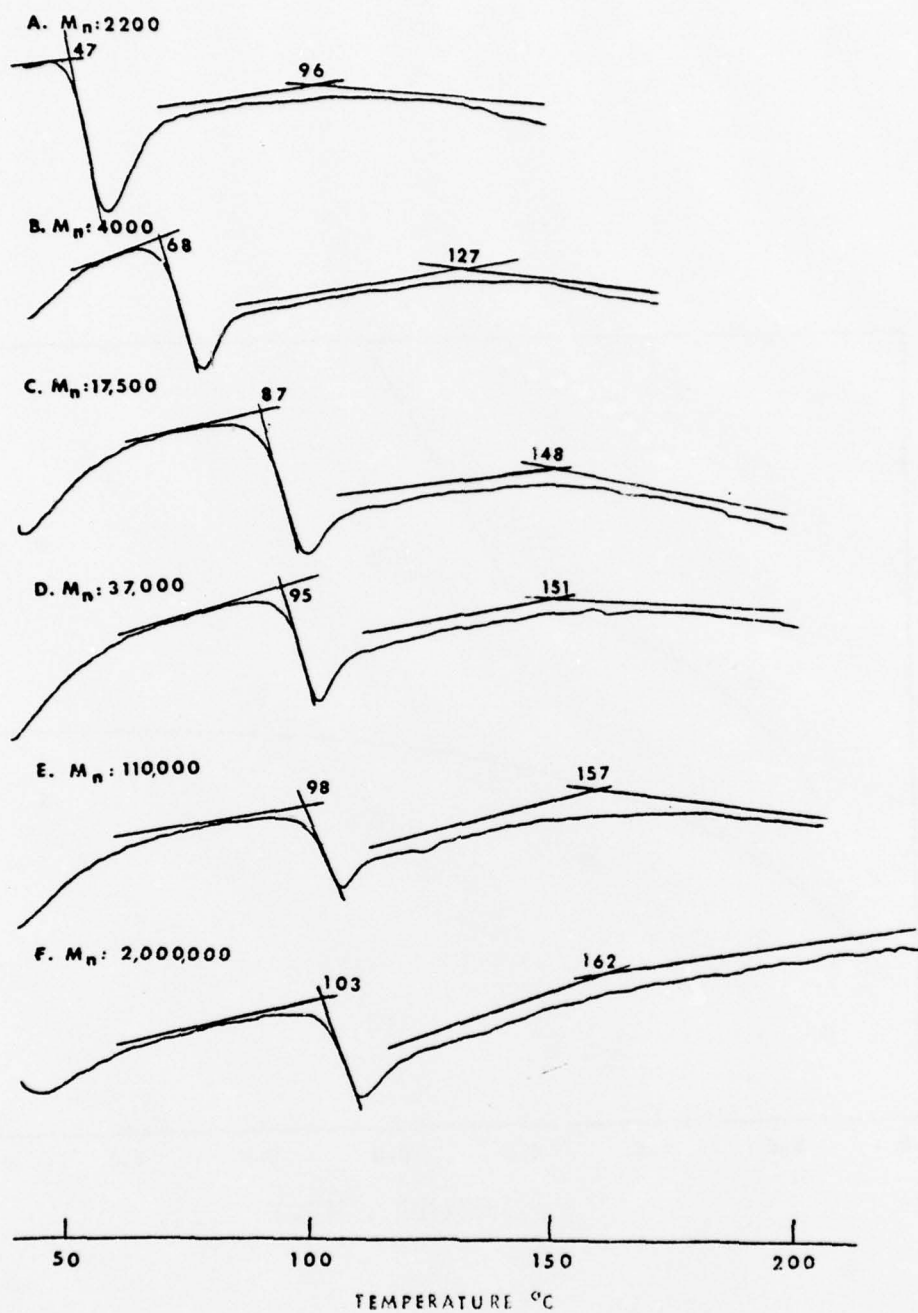


Fig. 21

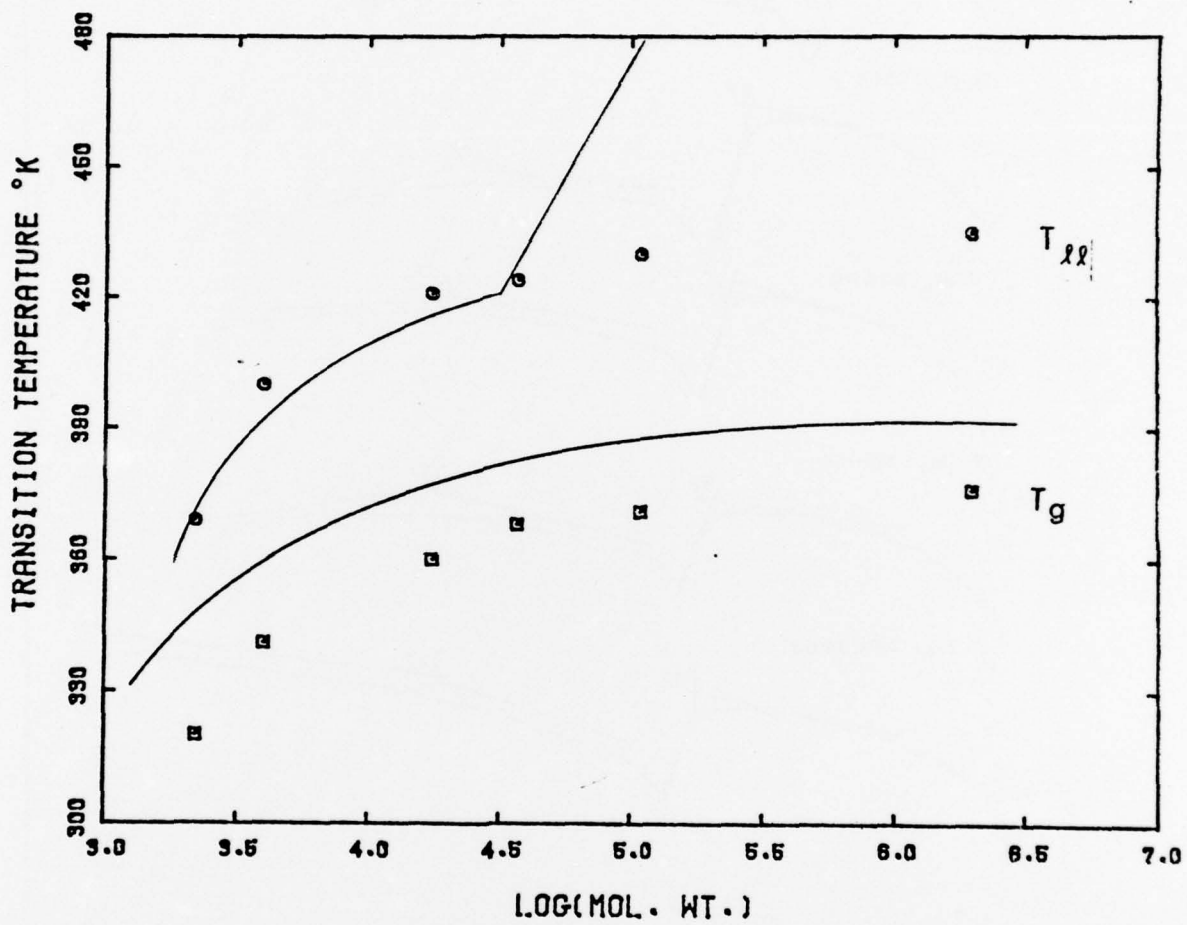


Fig. 22

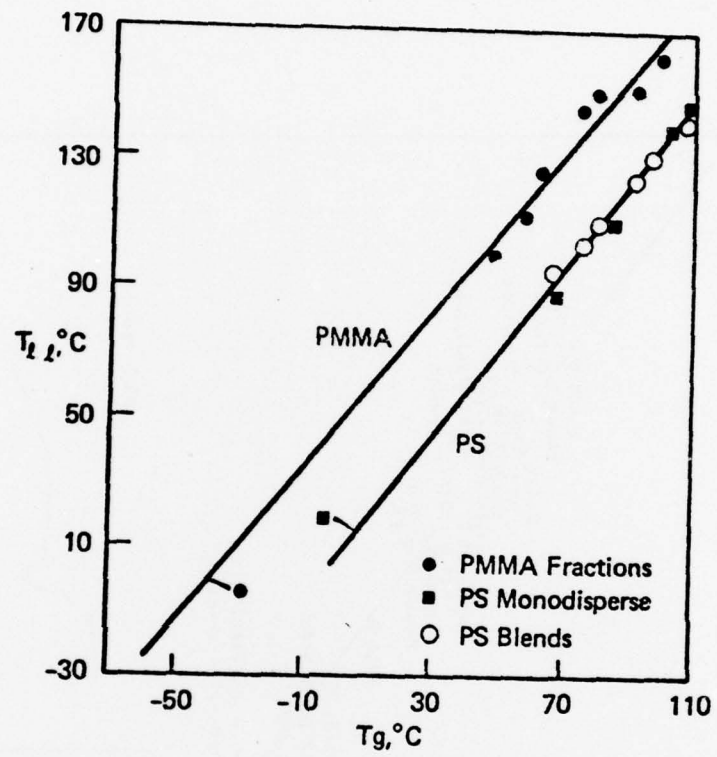


Fig. 23

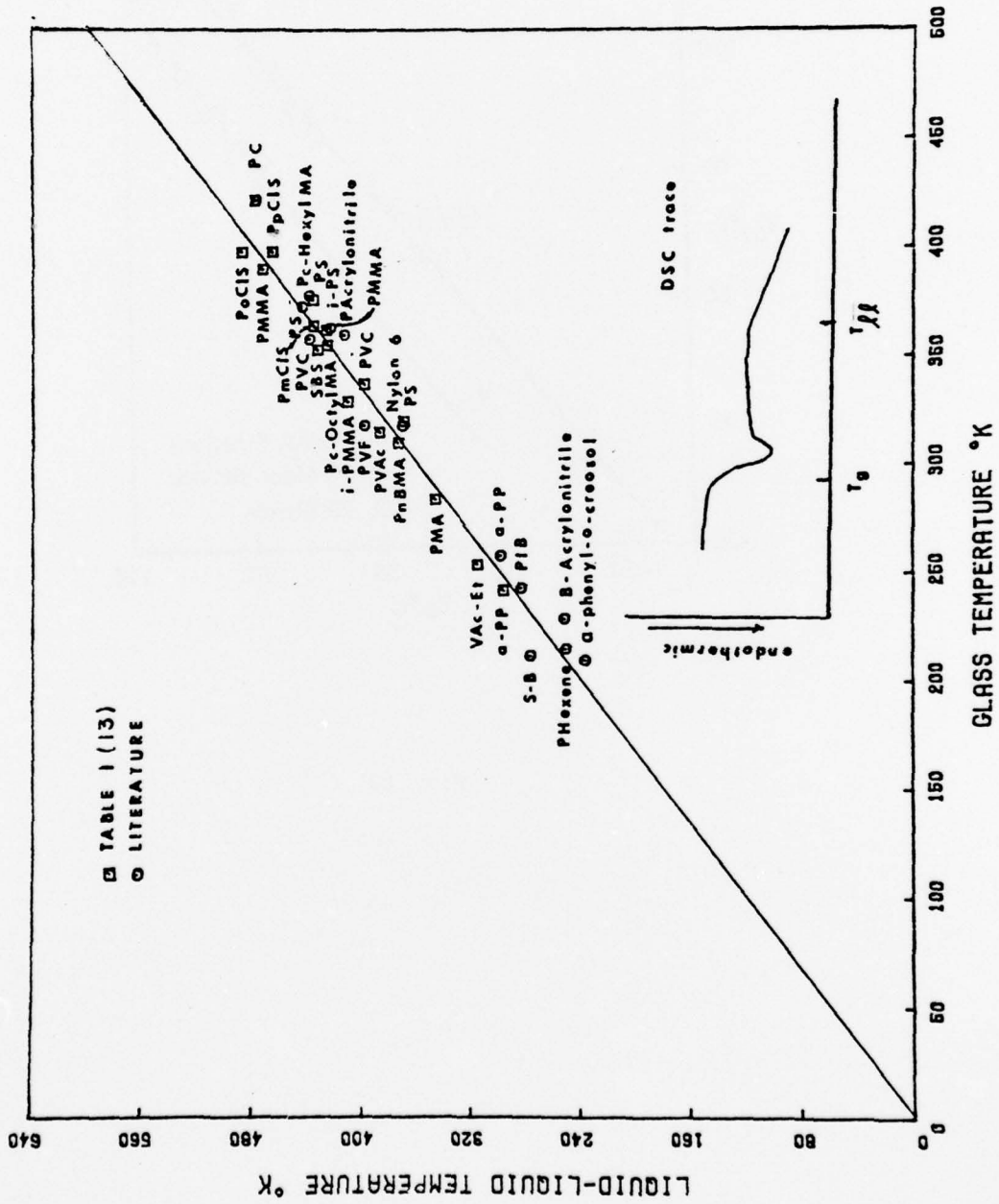


Fig. 24

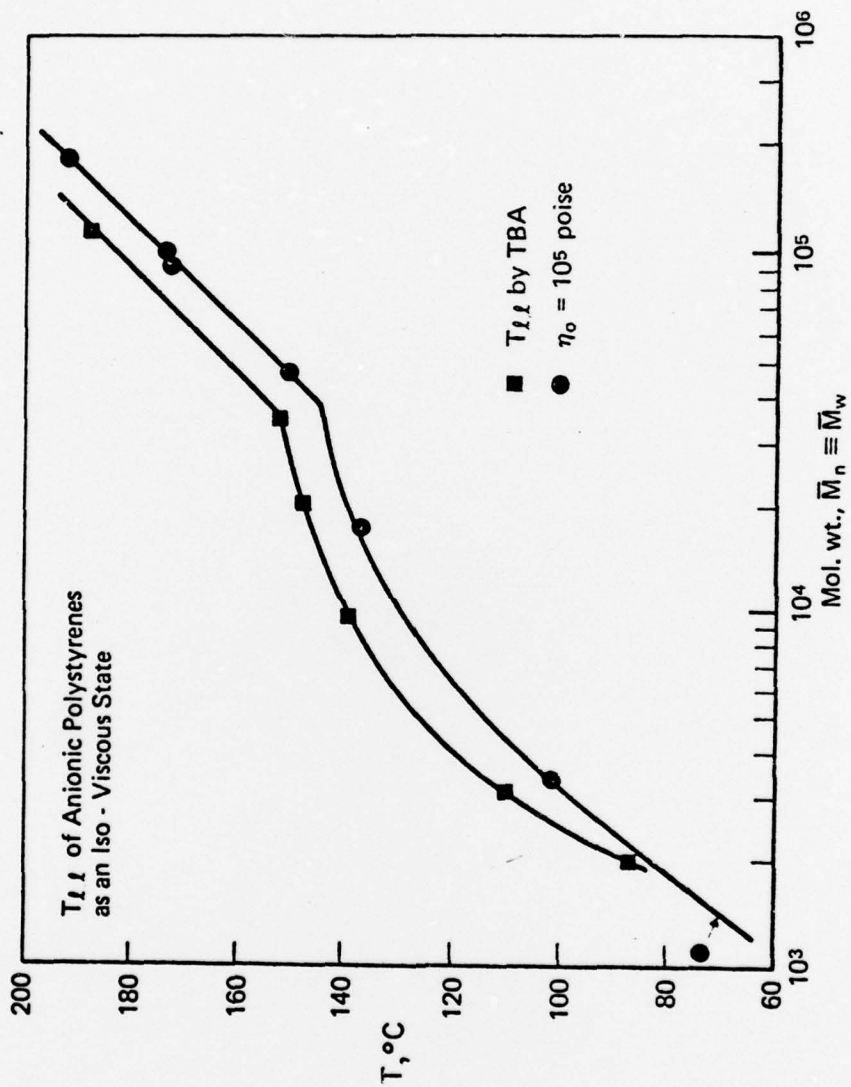


Fig. 25

REPORT DOCUMENTATION PAGE		READ INSTRUCTIONS BEFORE COMPLETING FORM
1. REPORT NUMBER Technical Report #11	2. GOVT ACCESSION NO.	3. RECIPIENT'S CATALOG NUMBER
4. TITLE (and Subtitle) The $T_{ll}$ Relaxation of Polystyrene ,	5. TYPE OF REPORT & PERIOD COVERED Technical Report , March 1976 - April 1977	6. PERFORMING ORG. REPORT NUMBER
7. AUTHOR(s) J. K. Gillham and R. F. Boyer	8. CONTRACT OR GRANT NUMBER(s) N00014-76-C-0200	9. PERFORMING ORGANIZATION NAME AND ADDRESS Polymer Materials Program Department of Chemical Engineering Princeton University, Princeton, N. J. 08540
10. CONTROLLING OFFICE NAME AND ADDRESS Office of Naval Research 800 North Quincy Street Arlington, Va 22217	11. REPORT DATE June 1977	12. PROGRAM ELEMENT, PROJECT, TASK AREA & WORK UNIT NUMBERS Task Number NR 356-504
13. MONITORING AGENCY NAME & ADDRESS (if different from Controlling Office) John K. / Gillham Raymond F. / Boyer	14. NUMBER OF PAGES 60	15. SECURITY CLASS. (of this report)
16. DISTRIBUTION STATEMENT (of this Report) Approved for Public Release; Distribution Unlimited.	17. SECURITY CLASS. (of this report)	18. DECLASSIFICATION/DOWNGRADING SCHEDULE
17. DISTRIBUTION STATEMENT (of the abstract entered in Block 20, if different from Report)	18. SUPPLEMENTARY NOTES	
18. SUPPLEMENTARY NOTES	19. KEY WORDS (Continue on reverse side if necessary and identify by block number) Polystyrene Transitions Torsional Braid Analysis Differential Thermal Analysis	
19. KEY WORDS (Continue on reverse side if necessary and identify by block number)	20. ABSTRACT (Continue on reverse side if necessary and identify by block number) A review of recent work by the authors on a relaxation ( $T_{ll}$ ) above the glass transition ( $T_g$ ) of amorphous polystyrene is presented. On the basis of experimental data from torsional braid analysis (TBA), differential scanning calorimetry (DSC) and differential thermal analysis (DTA), and of an examination of the literature, it is suggested that $T_{ll}$ represents a molecularly-based transition.	

LR